Master Thesis, Department of Geosciences

Pre-Jurassic evolution of the Fingerdjupet Subbasin, SW Barents Sea

Audrius Norkus

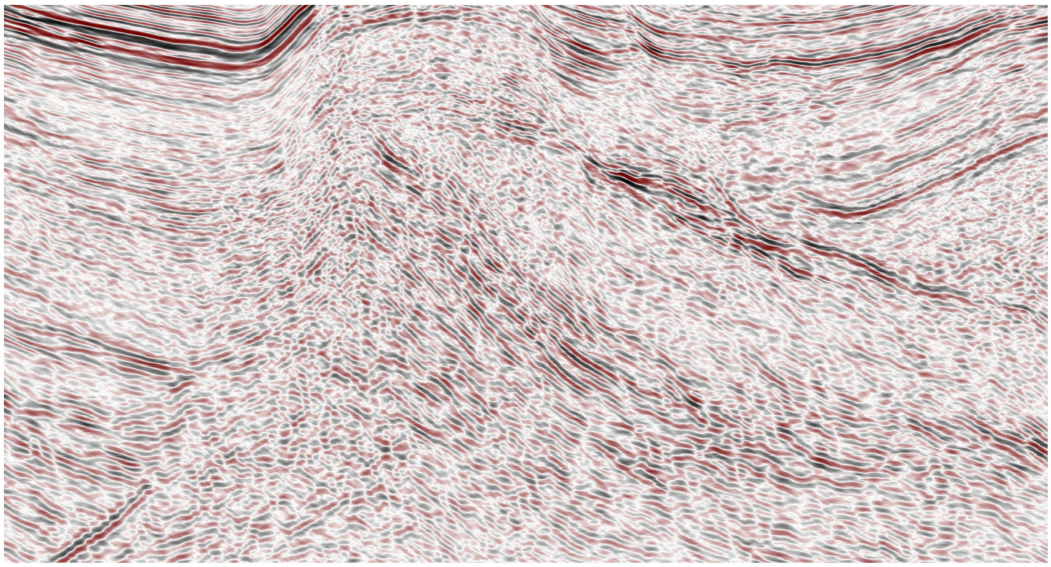

UNIVERSITY OF OSLO

FACULTY OF MATHEMATICS AND NATURAL SCIENCES

Pre-Jurassic evolution of the Fingerdjupet Subbasin, SW Barents Sea

Audrius Norkus

Master Thesis in Geosciences

Discipline: Petroleum Geology and Petroleum Geophysics

Department of Geosciences

Faculty of Mathematics and Natural Sciences

University of Oslo

June 2015

Abstract

The Fingerdjupet Subbasin is N-S trending basin in the western Barents Sea, which developed as a westward tilted halfgraben in the hanging-wall of a basin-bounding listric normal normal fault as a response to the extension in the North Atlantic during the Late Paleozoic. Thick succession from Carboniferous to Triassic contains complex geological evolution and using partial well control was examined during this study.

This thesis describes the pre-Jurassic structural and stratigraphic framework of the Fingerdjupet Subbasin. The interpretation of the 2D seismic lines was carried out using both software and paper method to obtain the detailed structural evolution of the basin and relate it to the sediment infill. Six seismic key lines were selected to represent the main structural and stratigraphic observations in the Fingerdjupet Subbasin. Based on the detailed interpretation of the succession from mid Carboniferous to Early Cretaceous, three megasequences were defined and described in detail to reconstruct the evolution of the basin through time. Based on megasequences time-thickness maps were created to study the lateral and vertical changes in the geometries and depositional patterns. These maps are presented together with time-structure maps with interpreted faults in order to relate the basin infill with the observed tectonic regimes in the area. Finally, the pre-Jurassic geological evolution is discussed with the focus on a regional setting and surrounding areas to recover the Fingerdjupet Subbasin evolution.

During the Late Paleozoic times, the Fingerdjupet Subbasin might have experienced three different extensional regimes. These were dated to be of Devonian (?), mid Carboniferous and late Permian age. Gabrielsen et al. (1990) suggested that the Fingerdjupet Subbasin formed during the Early Cretaceous due to the extension in the North Atlantic. However, after this study it can be suggested that the onset of the formation was in late Permian.

Acknowledgements

I would like to express my sincere gratitude to my supervisors, Professor Jan Inge Faleide, Professor Emeritus Johan Petter Nystuen, and Associate Proffesor Ivar Midtkandal, for their continued guidance and support over the past half a year. You are all wise men in your fields and I am grateful to have been able to learn from and work along side you all.

Special thanks also to the Department of Geosciences for creating a truly productive and balanced atmosphere in which to work in. It has been an inspiring experience to work with both the professional staff and the students of this department.

Additionally, I would like to give special thanks to TGS and Fugro for making the seismic data available.

Also, I would like to thank Senior Engineer Michael Heeremans for preparing the dataset and solving all the technical issues.

Contents

Chapter 1

Introduction

The Barents Sea is a marginal sea of the Arctic Ocean, which is a part of continental shelf of northwestern Eurasian continental plate. The epicontinental sea is bounded by the Eurasian Arctic Basin in the north, by the Novaya Zemlya in the east, by Fennoscandia and Russia in the south and southeast, and by the Norwegian – Greenland Sea in the west (Fig. **??**). The regional structuring and basin evolution has been discussed widely by previous workers (Faleide et al., 1984; Rønnevik and Jacobsen, 1984; Gabrielsen et al., 1990; Faleide et al., 1993b,a; Gudlaugsson et al., 1998) Generally, the eastern part was mainly influenced by the Late Paleozoic tectonism and minor deformations in post-Jurassic times, while the most intensive tectonism in the western part occurred in Late Mesozoic and Cenozoic times. Therefore, tectonism, basin formation, and rifting was propagating from east to the west throughout the Barents Sea during the geological history.

The main objective of this thesis is to study and understand the pre-Jurassic succession of the Fingerdjupet Subbasin with an emphasis on structural setting, timing and style of faulting and its influence on basin architecture and infill history. The Fingerdjupet Subbasin is a shallow basin where the succession from Carboniferous to Early Cretaceous is buried at a relatively shallow depth compared with other part in the SW Barents Sea and detailed geological investigation can be performed.

2D seismic data and four exploration wells located in the Fingerdjupet Subbasin and on the Norvarg Dome were used for interpreting the succession from mid Carboniferous to Early Cretaceous. Interpretation was carried out using Petrel software and particular lines were interpreted on paper to better understand the geological configuration of the Fingerdjupet Subbasin. The interpreted succession was subdivided into three megasequences and time-thickness maps were generated to define the history of basin infill and lateral vertical variations in thickness. Interplay between stratigraphy and structuring in the Fingerdjupet Subbasin will be presented throughout this work.

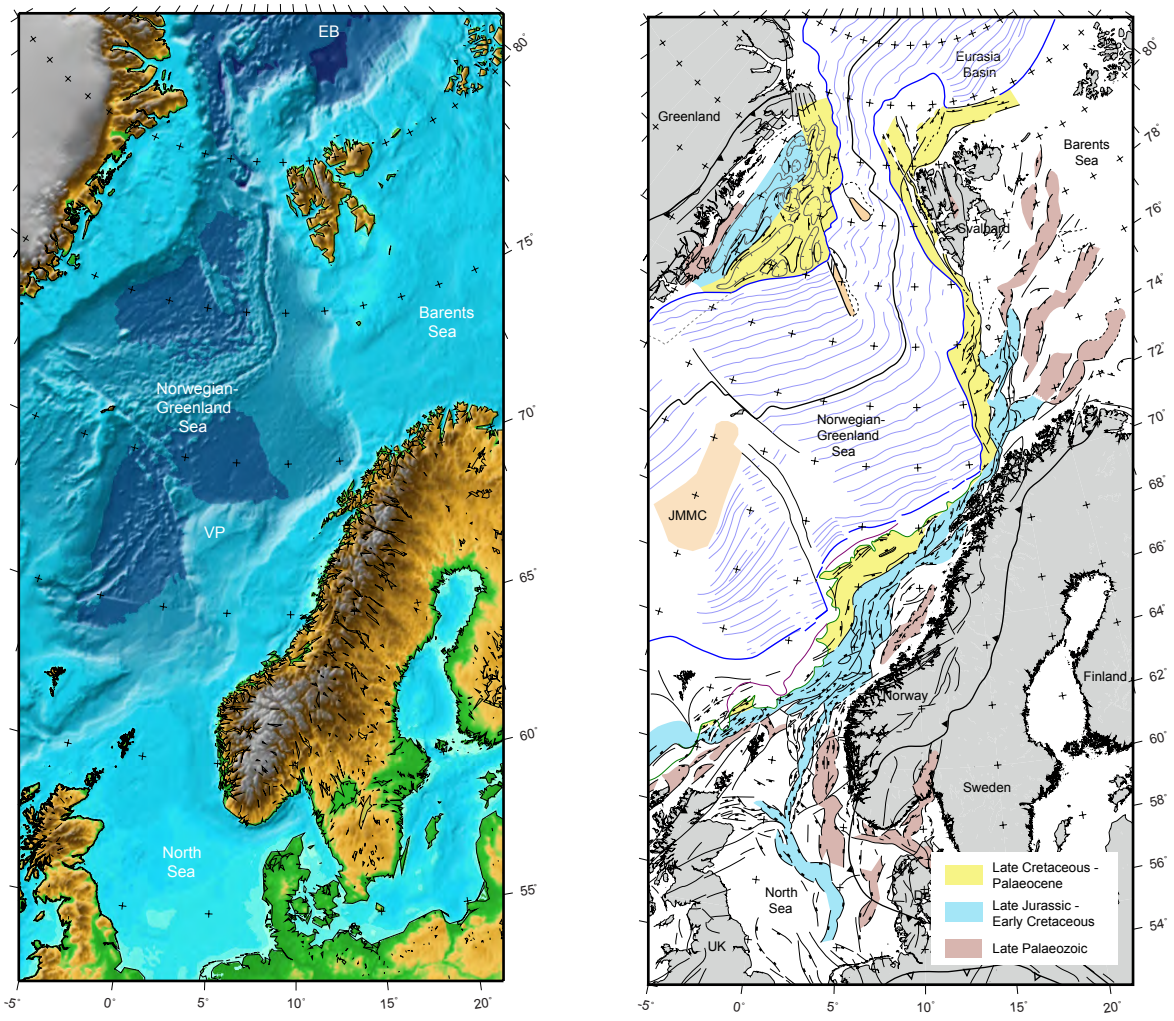

FIGURE 1.1: Regional setting and location of the study area. Figure on the left indicates the structural elements in the Barents Sea, the Norwegian Sea and the North Sea modified after Faleide et al. (2008)

.

Chapter 2

Geological framework

2.1 Regional geology

The Barents Sea is a marginal sea of the Artic Ocean, which is a part of the continental shelf of the northwestern Eurasian continental plate. The epicontinental sea is bounded by the Eurasian Arctic Basin in the north, by the Novaya Zemlya in the east, by Fennoscandia and Russia in the south and southeast, and by the Norwegian – Greenland Sea in the west. During the period from Late Paleozoic to Early Mesozoic times the epicontinental basin was bordered by the present – day Novaya Zemlya in the east, the Fennoscandian Shield to the south, the North American continent to the west and an open seaway to the northwest (Glørstad-Clark et al., 2011). The Barents Sea area can be subdivided into two major geological provinces that are separated by a huge monoclinal structure located in the central part. The geological evolution of the eastern part was affected by the Uralian Orogeny and the complex tectonics of Novaya Zemlya and the Timan-Pechora Basin. Processes that controlled the geology of the western province included post-Caledonian rifting events and later rifting episodes that lead to the continental break-up along the northwestern margin of the Eurasian plate (Smelror et al., 2009).

According to Faleide et al. (2010) the western Barents Sea can be subdivided into three discrete provinces (Fig. 2.1):

1. The Svalbard Platform which is overlain by comparatively flat-lying succession of Upper Palaeozoic and Mesozoic sediments, largely of Triassic age.

2. A region between the Norwegian coast and the Svalbard Platform, a platformal area that is composed of several highs and sub-basins with an accentuated structural relief towards the west. Sediments of Jurassic-Cretaceous and Palaeocene-Eocene age are present in the western part of the basins.

3. 3. A continental margin which is characterized by three main parts: a) a southern sheared margin along the Senja Fracture Zone; b) a central rifted complex related to volcanism

and located to the southwest of Bjørnøya Basin c) a northern, initially sheared and later rifted margin along the Hornsund Fault Zone.

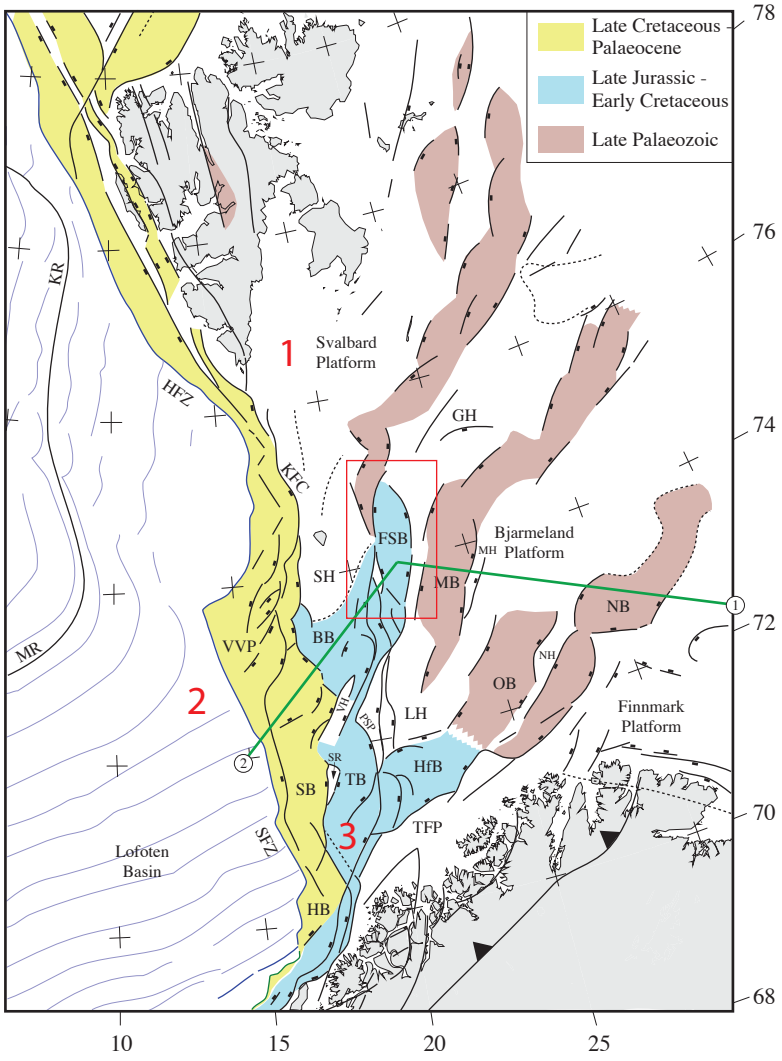

FIGURE 2.1: Structural elements in the western Barents Sea. Red rectangle - the target area of the research. Numbers 1-3 indicate three different regions in the western Barents Sea defined by Faleide et al. (2010). Green lines mark the extent of regional profiles, see Fig. 2.3 for full cross sections.

2.2 Structural evolution and stratigraphy

According to the crustal structure, tectonic style and sedimentary infill, three geological provinces are present in the SW Barents Sea. They are separated by the main Jurassic-Cretaceous faults (the Ringvassøy-Loppa Fault Complex, Leirdjupet Fault Complex, Bjørnøyrenna Fault Complex, and the Troms-Finnmark Fault Complex south of 71 °N) bordering the deep Cretaceous

basins, continental plate margin faults along the Senja Fracture Zone and the eastern boundary of the Vestbakken Volcanic Province. These three geological provinces comprise (Faleide et al., 1993a,b). These three geological provinces comprise:

1. The oceanic Lofoten Basin that was formed during the opening of the Norwegian-Greenland Sea in Paleogene times and the Vestbakken Volcanic Province;
2. The south-western Barents Sea basin province which contains deep Cretaceous and Early Cenozoic basins (Harstad, Tromsø, Bjørnøya and Sørvestsnaget basins) separated by intrabasinal highs (Senja Ridge, Veslemøy High and Stappen High);
3. Mesozoic basins and highs between 20 ° and 25 °E, which have not experienced the prominent Cretaceous-Paleogene subsidence (Finmark Platform, Hammerfest Basin, Loppa High, Fingerdjupet Subbasin).

The continental margin faults along the Senja Fracture Zone and the eastern boundary of the Vestbakken Volcanic Province together with the main Jurassic-Cretaceous faults (Troms-Finnmark Fault Complex south of 71 °N, the Ringvassøy-Loppa Fault Complex, Bjørnøyrenna Fault Complex and Leirdjupet Fault Complexes) bound these provinces.
The Barents Sea area has a complex geological framework formed by regional basins and highs. These were formed during two plate collision episodes followed by a continental separation. It is believed that most of the basement of the western Barents Sea is of Caledonian origin and derives from its metamorphic Archean – Proterozoic rocks and younger volcanic rocks (Ritzmann and Faleide, 2007). The crystalline-metamorphic basement formed during the Caledonian orogeny that culminated around 400 Ma years ago, when the Baltic plate (Scandinavia, western Russia) collided with the Laurentian plate (North America, Greenland). The Laurasian continent formed during the plate collision with the closing of the Iapetus Ocean that had separated Baltica from Laurentia since late Ediacaran time. Basement rocks of the eastern Barents Sea formed during a collision between the Western Siberia and the Laurasian continents approximately 240 Ma ago in the latest Permian – earliest Triassic. The suture zone of this closure is marked by the Ural Mountain Chain and its northern extension into Novaya Zemlya (Doré, 1995).

It is believed that the Caledonian basement structural setting has influenced later structural development of the area (Gudlaugsson et al., 1998; Ritzmann and Faleide, 2007). The western part of the region acted as a transfer zone linking spreading and rifting that happened in the North Atlantic and the Arctic realms due to the collapse of the Caledonian orogeny (Gudlaugsson et al., 1998). According to the new aeromagnetic data it has been proposed that the

Caledonian nappes well constrained onshore swing to from a NE-SW trend onshore Norway to NW-SE/NNW-SSE across the SW Barents Sea platform area. Moreover, the basement magnetic pattern could reflect the regional post-Caledonian development of the late Paleozoic basins (Gernigon and Brönner, 2012; Gernigon et al., 2014).

Most of the Barents Sea area was affected by crustal extension during Late Paleozoic times and this resulted in a fan-shaped array of block-faulted basins separated by highs (Rønnevik and Jacobsen, 1984; Gabrielsen et al., 1990; Gudlaugsson et al., 1998). Rift zones were established in the middle Carboniferous, its width reached 300 km and extended more than 600 km northeast (Faleide et al., 2010; Gudlaugsson et al., 1998). Rifting terminated in the late Carboniferous in the eastern areas, and the relief was filled by a platform succession of late Carboniferous-Permian age. It includes cyclical dolomites and evaporites passing into massive limestones. Carbonate sedimentation occurred in the entire region until late early Permian when a transition to clastic deposition started, due to erosion of the Ural Mountains in the southeast and landmasses to the south (Johansen et al., 1993; Faleide et al., 2010). Renewed faulting, uplift and erosion affected the western part of the rift system during the late Permian-early Triassic times (Faleide et al., 2010).

During the Triassic period large amounts of clastic sediments were deposited, which were transported into the Barents Sea from the Uralian highland in the east, Baltic Shield in the south-east, intrabasinal highs and the Laurentia continent to the west. Shales and sandstones dominated the successions from this period. A regional, rather deep water epicontinental basin covered most of the Barents Sea during the Early Triassic. The sea shallowed by sediment infill during the Triassic, and some parts of the large area were partially exposed. During the Middle Triassic, the continental regime dominated in large areas and regional basin was filled by the northward and westward prograding deltaic system. Late Triassic sediments were derived mainly from the northwest and the period culminated with regression and erosion (Riis et al., 2008; Faleide et al., 2010; Glørstad-Clark et al., 2010, 2011; Høy and Lundschien, 2011).

Sandstones dominate the succession from the Lower to Middle Jurassic in the Barents Sea. The late Middle Jurassic sequence boundary indicates the beginning of rifting in the SW Barents Sea and interaction between sea-level changes and continuous faulting reflected by the unconformities in the Upper Jurassic succession. Regional extension supplemented by strike-slip adjustments along old structural lineaments characterized the structuring of the SW Barents Sea in the Late Jurassic-earliest Cretaceous (Faleide et al., 2010).

Rifting continued throughout the Early Cretaceous times. The Lower Cretaceous strata are dominated by shales and claystones with thin layers of interbedded silt, limestone and dolomite,

which were deposited in marine environments with distal conditions and periodic restricted circulation. Widespread magmatism without any signs of faulting portrayed the northern part of the Barents Sea in the Early Cretaceous. Sills and dykes belonging to the regional High Arctic Large Igneous Province (HALIP) are documented from Svalbard, Franz Josef Land and off-shore areas in the northern Barents Sea. It was related to rifting and breakup in the Amerasia (Canada) Basin and the formation of the Alpha Ridge (Faleide et al., 2010).

The two-stage opening of the Norwegian-Greenland Sea and the formation of the sheared western Barents Sea continental margin were dominant factors in the formation of the Cenozoic structural setting. These tectonics movements gave a rise to a rapid Late Paleocene subsidence. During the Cenozoic uplift and erosion around 1000 – 1500 m of sedimentary strata were eroded in the SW Barents Sea (Faleide et al., 2010).

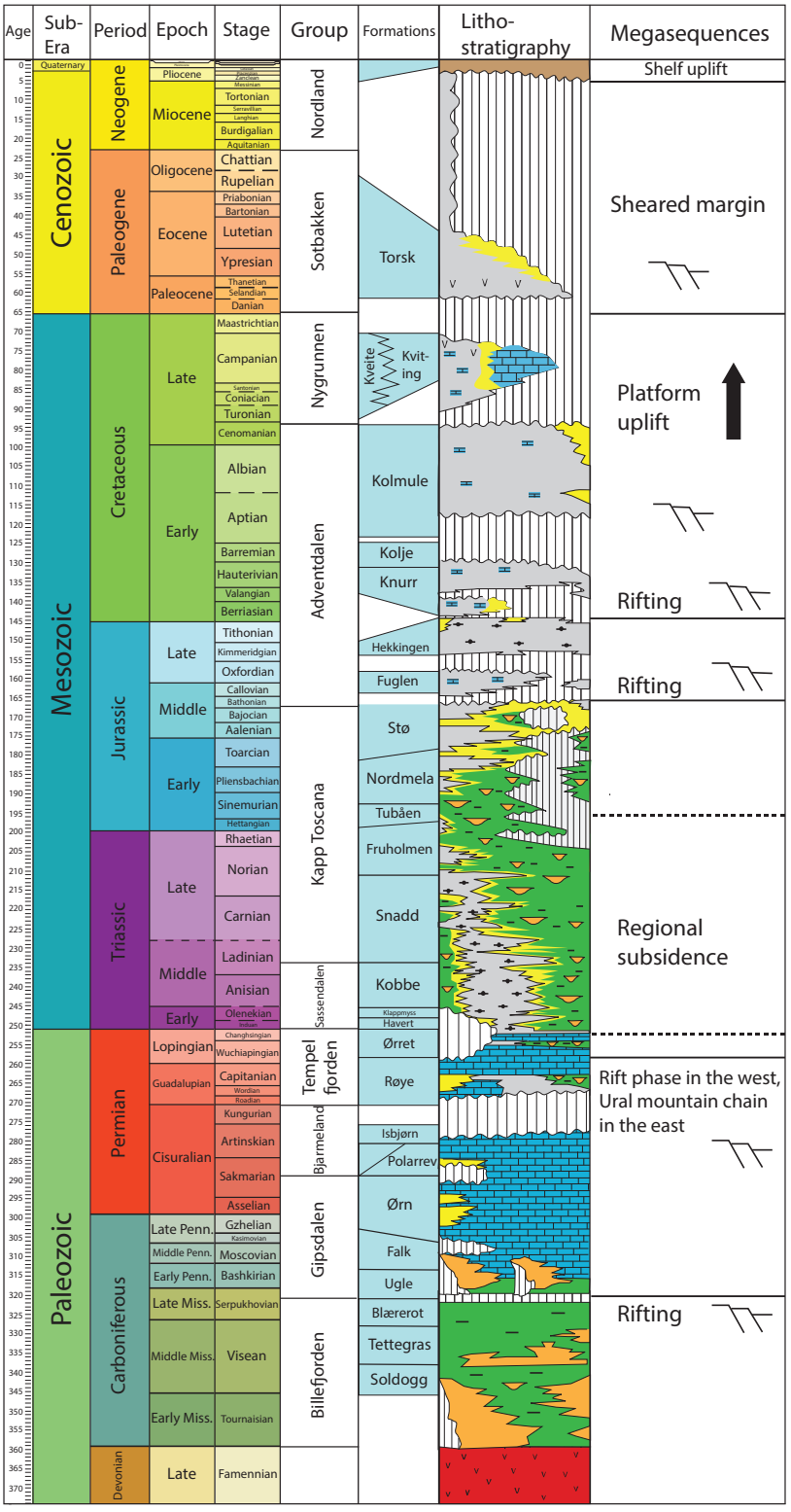

FIGURE 2.2: Lithostratigraphy of the western Barents Sea with major tectonic events. Modified after Glørstad-Clark et al. (2010).

2.3 Main structural elements

2.3.1 The Loppa High

The Ringvassøy-Loppa and Bjørnøyrenna Fault complexes bound the Loppa High on the west. The northeastern limit of the high is marked by a major salt structure, the Svalis Dome, and its associated rim syncline, the Maud Basin. To the east and southeast, the Loppa High is bordered by a monocline towards the Hammerfest Basin and the Bjarmeland Platform, and on the south by the Asterias Fault Complex (Gabrielsen et al., 1990).

The high is a result of Late Jurassic to Early Cretaceous and Late Cretaceous-Paleogene tectonism. Its western crest was rejuvenated as a high at least four times since Devonian. During the period from Ladinian to Callovian, the high together with the Hammerfest Basin and Bjarmeland Platform formed a regional cratonic platform. During most of the Cretaceous the Loppa High was an island with deep canyons cutting into the Triassic succession in the high. Most of the Palaeogene shales that used to cover the high were eroded during the Late Cenozoic uplift (Gabrielsen et al., 1990).

2.3.2 The Bjarmeland Platform

The Bjarmeland Platform is bounded by the Sentralbanken and Gardarbanken highs in the north, the Fingerdjupet Subbasin and the Loppa High in the west and the Hammerfest and Nordkapp basins in the south and southeast. The platform contains the Svalis, Samson and Norvarg domes, the Swaen Graben, the Maud Basin, the Norsel and Mercurius highs, and parts of the Hoop Fault Complex. It is assumed that Palaeozoic and Precambrian rocks, which dip gently to the south due to Late Cenozoic uplift, cover platform area. Progressively older sediments subcrop to the north at the unconformity at the base of the Quaternary (Gabrielsen et al., 1990).

The Bjarmeland Platform started to develop in Late Carboniferous as a stable platform. During the period from Late Permian to Early Triassic it was possibly terminated by the fault zone oriented north-south in its western part. A distinct structural high, with the same orientation, existed in the east of the fault zone throughout the Late Permian and Early Triassic. The transition from pre-platform to a platform development is interpreted in the boundary between Early Carboniferous clastic sediments and Late Carboniferous to Permian carbonates. Throughout Late Triassic times, the platform, with a concentrated Lower to Middle Triassic succession, was transformed into a basin with the thickest sediments of Upper Triassic age. The present Loppa

High and Fingerdjupet Subbasin were initiated by the Late Mesozoic and Paleogene tectonism and now characterize the western termination of the Bjarmeland Platform. The structural pattern of the Bjarmeland Platform is mostly related to the weak extension and salt tectonics (Gabrielsen et al., 1990).

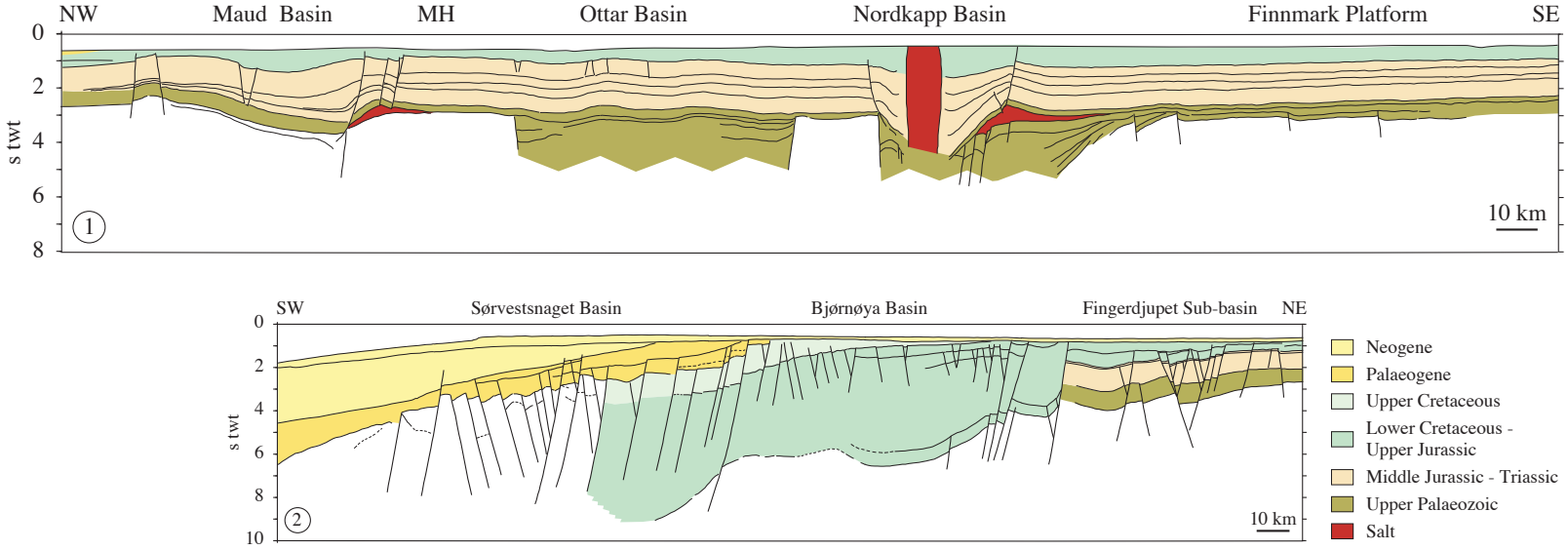

FIGURE 2.3: Regional profiles across the western Barents Sea (Faleide et al., 2010). See Fig. 2.1 for location.

2.3.3 The Bjørnøya Basin

The Bjørnøya Basin is divided into a deeper western part and a shallower eastern part (the Fingerdjupet Subbasin) by the Leirdjupet Fault Complex and has a NE-SW trend. The basin is confined by the Bjørnøyrenna Fault Complex in the southeast and its northwestern boundary is a faulted slope dipping down from the Stappen High towards the basin. Hence, certain characteristics of a half graben are present in the Bjørnøya Basin (Gabrielsen, 1984). Faleide et al. (1984) interpreted some of the dome structures present in the Bjørnøya Basin as salt diapirs. However, it was concluded that no salt diapirs exist there (Rønnevik and Jacobsen, 1984). According to the other reflection seismic data in the area, salt structures can only be present at great depths (Gabrielsen et al., 1990).

The Bjørnøya Basin is principally related with the Early Cretaceous subsidence, which had influenced a large area to the north. The basin was affected by local inversion and faulting linked to the Stappen High and the Bjørnøyrenna Fault Complex in the Late Cretaceous and Paleogene, when its tilted northern margin was formed. Due to tilting present in the area, it has to be considered whether the Bjørnøya Basin is a true half-graben or currently observed half-graben geometry is a secondary effect of inversion. The history of the basin before the Early Cretaceous is not well known, nevertheless Ziegler (1988) based on gravimetric measurements, which could indicate the presence of a palaeobasin prior the present Bjørnøya Basin, suggested that it was active in Late Carboniferous to Permian time (Faleide et al., 1984; Rønnevik and Jacobsen, 1984; Faleide et al., 1993b; Gabrielsen et al., 1990).

2.3.4 The Fingerdjupet Subbasin

The Fingerdjupet Subbasin, according to Gabrielsen et al. (1990) is the shallow northeastern part of the Bjørnøya Basin. In the west and south it is bordered by the Leirdjupet Fault Complex, by the Loppa High in the southeast and the Bjarmeland Platform in the east. The subbasin contains a horst and graben pattern, which is outlined by a system of NNE-SSW trending fault blocks (Gabrielsen et al., 1990).

The Fingerdjupet subbasin was formed in Early Cretaceous, while the dominant fault trend was created during the Late Jurassic tectonism. Several major faults were reactivated in Cretaceous and probably Cenozoic times. It is believed that during the period from the Ladinian to Callovian, the subbasin was a part of the regional cratonic platform present at that time in the area. Pre-Ladinian history is similar to that of the Loppa and Stappen highs. However, a thick, Late

Permian sedimentary sequence may be present in the subbasin. Subsidence of the Fingerdjupet subbasin started from Early Cretaceous times as a consequence of Late Jurassic to Early Cretaceous extensional tectonic episode. During the Late Cenozoic erosion, a sequence of at least 2000 m was eroded, therefore the Cenozoic history of the subbasin is unknown (Gabrielsen et al., 1990).

2.3.5 The Leirdjupet Fault Complex

The Leirdjupet Fault Complex is orientated N-S direction and is separating the deep part of the Bjørnøya Basin from the shallower Fingerdjupet Subbasin. In the north, the structure separates into several faults with smaller normal throws. This northern part is described as rotated fault blocks. In the south, the complex is outlined by a single fault, which has a large throw towards the Bjørnøya Basin and has been related with dragging and flexures (Gabrielsen et al., 1990).

Different fault elements of the complex were active during numerous episodes. It is thought that main movements occurred in the (early?) Carboniferous, mid Jurassic and Early Cretaceous. Moreover, faults may have been active in Late Cretaceous or Cenozoic times. Furthermore, minor movements can be followed in the Triassic and possibly in the latest Carboniferous to Permian (Gabrielsen et al., 1990; Bjørnestad, 2012).

2.3.6 The Bjørnøyrenna Fault Complex

The Bjørnøyrenna Fault Complex is oriented NE-SW and separates the shallow Fingerdjupet Subbasin from the Loppa High in the northeast and in the southeast it delineates the boundary between the Loppa High and the Bjørnøya Basin. The fault complex is terminated in the northeastern part where the Fingerdjupet Subbasin can no longer be traced and in the south by the northern part of the Tromsø Basin (Gabrielsen et al., 1990).

The fault complex was tectonically active during the period from Late Jurassic to Early Cretaceous and reactivation occurred in Late Cretaceous and Paleogene times. It is defined by normal faults with large throws, where in some places it is related with dome structures. Nevertheless, signs of inversion are present, with reverse faults and strong deformation of the footwall blocks and deformed fault planes. The vertical displacement throughout the Bjørnøyrenna Fault Complex reaches up to 6 seconds TWT as defined at Upper Triassic levels. However, the throw reduces towards north and south (Gabrielsen et al., 1990).

2.4 General outline of the stratigraphy

A brief description of the formations in the sedimentary succession interpreted in this study ranging from the top of Billefjorden Group in the Carboniferous to Base Cretaceous Unconformity is given below.

Gipsdalen Group

The lower part of the group is composed of siltstones, red-bed sandstones and conglomerates while limestones and dolomites with minor occurrences of evaporites in the platform areas dominate the upper part. Age is expected to be from Late Carboniferous to Early Permian (Larssen et al., 2002).

Ugle Formation. Dominant lithology is coarse-grained sandstones, reddish-brown to brown conglomerates and minor siltstones. The depositional environment is interpreted as arid to semi-arid terrestrial due to the domination of red-coloured sediments and the nonexistence of marine fossils (Larssen et al., 2002).

Falk Formation. Lithology of the formation can be described as a mixture of shallow-marine sandstones and carbonates, and marine siltstones. Sediments deposited as a response to high-amplitude and high frequency sea level fluctuations (Larssen et al., 2002).

Ørn Formation. Shallow marine carbonates are dominating on the platform areas when interbedded carbonates and evaporites are present in the more distal ramp to basinal settings. Depositional environment is interpreted to be the same as in Falk Formation (Larssen et al., 2002).

Bjarmeland Group

Siliciclastic rocks are rare and white to light grey limestones containing cool-water fauna of bryozoans, brachiopods, crinoids and siliceous sponges is the dominant lithology. Age of the group is defined as Early Permian (Larssen et al., 2002).

Polarrev Formation. It is composed of white to light grey, massive to thickly bedded limestone. The lower part of the formation is dominated by more thin-bedded silty limestones. It was deposited in a range of subenvironments, within a bryozoan-dominated bioherm complex (Larssen et al., 2002).

Isbjørn Formation. It is dominated by white to light grey bioclastic limestones (wackestone to grainstone) with fauna mainly of crinoids and bryozoan. Chert nodules occur infrequently in the whole section. Sedimentary environment was interpreted as inner shelf (Larssen et al., 2002).

Tempelfjorden Group

The group is composed of fine-grained siliciclastics containing silt/sandstones, shales, marls, calcareous claystones and silicified skeletal limestones. It was deposited during the period from mid until late Permian (Larssen et al., 2002).

Røye Formation. Silicified sediments dominate the formation as the result of early silicification processes that were sourced by abundant silica sponge spicules. The lower part of the formation is dominated by dark grey to black, silicified calcareous claystone and traces of organic material while the upper part of the formation consists of bryozoan-dominated limestone (wackestone to grainstone), silicified carbonate mudstone, silicified marl, calcareous claystone, interbedded spiculite and spiculitic chert. Depositional environment of the lower part was interpreted as distal marine environment. The middle to upper parts of the formation represent distal marine, moderate to deep shelf setting (Larssen et al., 2002).

Ørret Formation. Sandstones, siltstones and shales dominate the formation. Sandstones are fine-grained and appear as isolated thin beds separated by shales. Limestone beds are rare in the formation. Deposition took place in deltaic, lower coastal plain, deep shelf environments where dysoxic to anoxic conditions occurred locally in the eastern part (Larssen et al., 2002).

Sassendalen Group

The dominant lithology is grey to black claystones and shales with grey siltstones and sandstones in the upper part. The group was deposited from Early to Middle Triassic times (Dalland et al., 1988).

Havert Formation. Formation is composed of medium to dark grey shales with interbedding pale grey sandstones and siltstones, which form two coarsening upwards sequences. The depositional environment is interpreted as marginal to open marine with evidences of coastal settings in the southeast or south (Dalland et al., 1988).
Klappmyss Formation. It is dominated by dark grey shales, which in the upper part are interbedded with sandstones and shales. Sedimentation took place in marginal to open marine environments (Dalland et al., 1988).
Kobbe Formation. Lower part of the formation consists of 20 m thick shale unit while upper part is formed of interbedded carbonate cemented sandstone, shale and siltstone. Transgressive rhythm mark the sedimentation of the lower part of the formation and upper part was formed when clastic marginal marine sedimentation was renewed from southern coastal areas (Dalland et al., 1988).

Kapp Toscana Group

Shales with thin intervals of coals dominate the lower part while the upper part is mainly composed of pale grey sandstones. The age is suggested from Middle Triassic to late Early Jurassic (Dalland et al., 1988).

Snadd Formation. Grey shales dominate the lower part of the formation, where the upper part consists of interbedded grey siltstones and sandstones. Limestones and calcareous beds can be observed in the lower and middle parts of the formation and coaly lenses are present in the upper part. Moreover, red-brown shales can be found near the top of the unit. Sedimentation environment is interpreted as distal marine, with storm-derived sands and silts and large-scale prograding deltaic system (Dalland et al., 1988).
Fruholmen Formation. Formation is dominated by interbedded grey to dark grey shales and coals in the lower part and shales with sandstones in the upper part. Middle part of the formation is dominated by sand. Shales formed in open marine environment while sandstones are of fluvial or coastal origin (Dalland et al., 1988).
Nordmela Formation. It is formed of interbedded shales, claystones, siltstones, sandstones that become more abundant towards the top and minor coals (Dalland et al., 1988).
Stø Formation. The formation is dominated by moderately to well-sorted sandstones with

thin units of shale and siltstone. Some wells consist of phosphatic lag conglomerates, particularly in upper parts of the unit (Dalland et al., 1988).

Adventdalen Group

It is composed of marly dolomitic limestones with thin interbeds of shales and claystones in the lower part and dark grey shales and claystones with interbedded siltstone, limestone and dolomite in the upper part. The group was deposited from late Early Jurassic until late Early Cretaceous (Dalland et al., 1988).

Fuglen Formation. In the type well the formation consists of pyritic dark brown mudstones with interbedded thin white to brownish grey limestones (Dalland et al., 1988).
Hekkingen Formation. Brownish-grey to very dark grey shale and claystone dominate with infrequent thin interbeds of sandstone, siltstone, limestone and dolomite (Dalland et al., 1988).
Knurr Formation. It is formed of dark grey to greyish brown claystone with interbeds of thin dolomite and limestone present. Thin sandstones can be observed in the lower part of the formation where red to yellow brown claystone usually occur in the upper parts of the unit (Dalland et al., 1988).
Kolje Formation. The formation is dominated by dark brown to dark grey shale and claystone with thin units of pale limestone and dolomite. Thin interbeds of grey-brown siltstone and sandstone are present in the upper part of the formation (Dalland et al., 1988).
Kolmule Formation. Dark grey to green claystone and shale, silty in parts, are dominating. Minor thin siltstone interbeds with limestone and dolomite stringers and occurring traces of glauconite and pyrite are present (Dalland et al., 1988).

Chapter 3

Seismic Interpretation

3.1 Data and methods

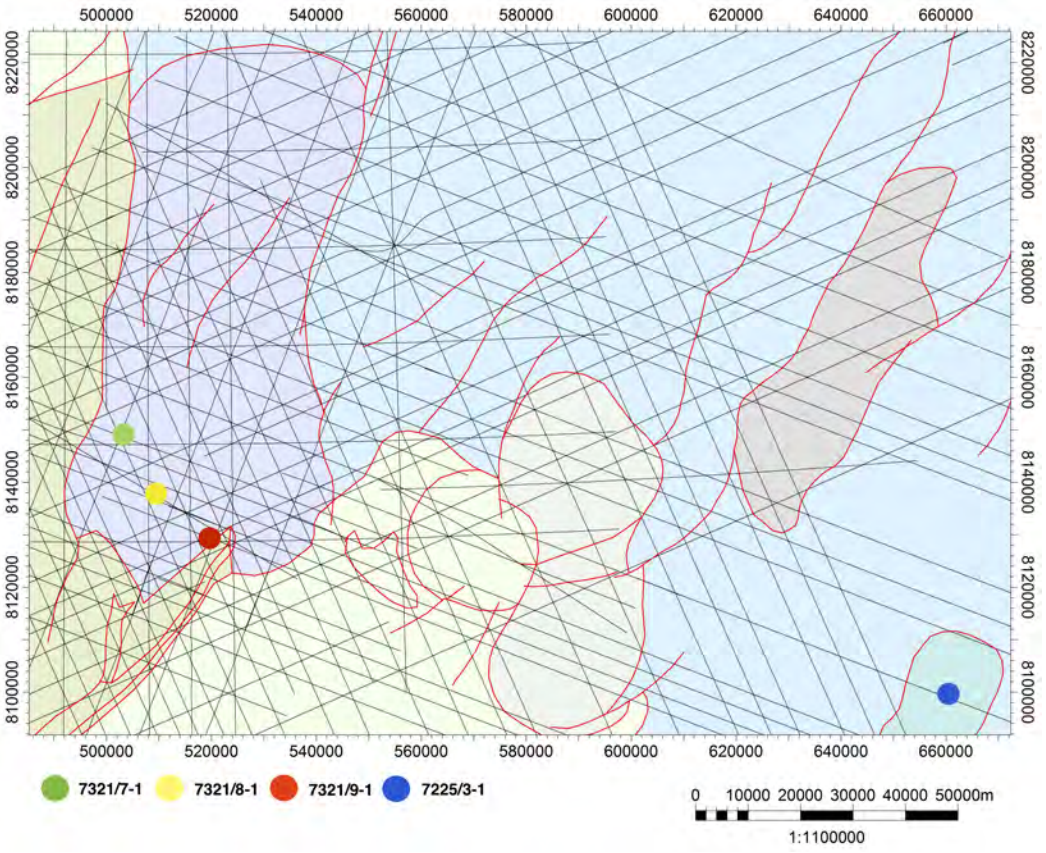

FIGURE 3.1: 2D seismic lines and three exploration wells that were used during this thesis. Map modified after Norwegian Petroleum Directorate (2015).

The dataset used in this study comprises 2D reflection seismic lines of multiple surveys with varying lateral and vertical resolution. In order to tie the lithostratigraphy with the seismic data in the area of interest four exploration wells were used (7321/7-1, 7321/8-1, 7321/9-1, 7225/3-1). Wells 7321/7-1, 7321/8-1, 7321/9-1 are located in the southern part of the Fingerdjupet Subbasin, north-west of the Loppa High and east of the Bjørnøya Basin. Well 7225/3-1, situated

on the Norvarg Dome, was used to tie the deeper levels of importance that were not penetrated by the wells in the Fingerdjupet Subbasin.

				Wells			
Era	Period	Gp	Fm	7321/7-1	7321/8-1	7321/9-1	7225/3-1
Cenozoic	Neogene	Nordland	-	499	491	483	-
Mesozoic	Cretaceous	Adventdalen	Kolmule	526	546	558	416
			Kolje	1892	1352	986	636
			Knurr	1918	1383	1317	670
	Jurassic		Hekkingen	1965	1427	1367	695
			Fuglen	1999	1437	1379	727
		Kapp Toscana	Stø	1999	1437	1379	727
			Nordmela	2022	1455	1417	-
	Triassic		Fruholmen	2039	1467	1424	770
			Snadd	2207	1626	1572	804
			No formal name	-	-	-	1146
		Sassendalen	Kobbe	-	-	-	1522
			Klappnyss	-	-	-	2155
			Havert	-	-	-	2555
			Undifferentiated	-	3362	-	-
Paleozoic	Permian	Tempelfjorden	Ørret	-	-	-	3666
			Røye	-	3398	-	3771
		Bjarmeland	Isbjørn	-	-	-	3931

TABLE 3.1: Four exploration wells used in the research with their lithostratigraphic units and total depth in meters (Norwegian Petroleum Directorate, 2015).

3.2 Seismic interpretation procedures

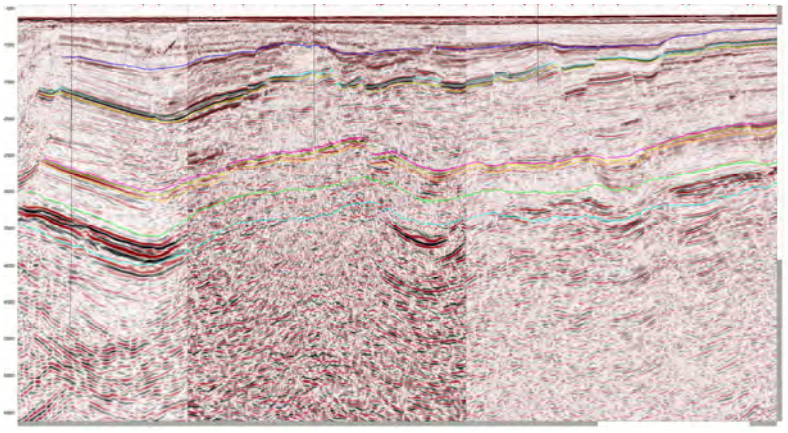

FIGURE 3.2: Composite line going through the exploration wells 7321/7-1, 7321/8-1 and 7321/9-1 in the Fingerdjupet Subbasin.

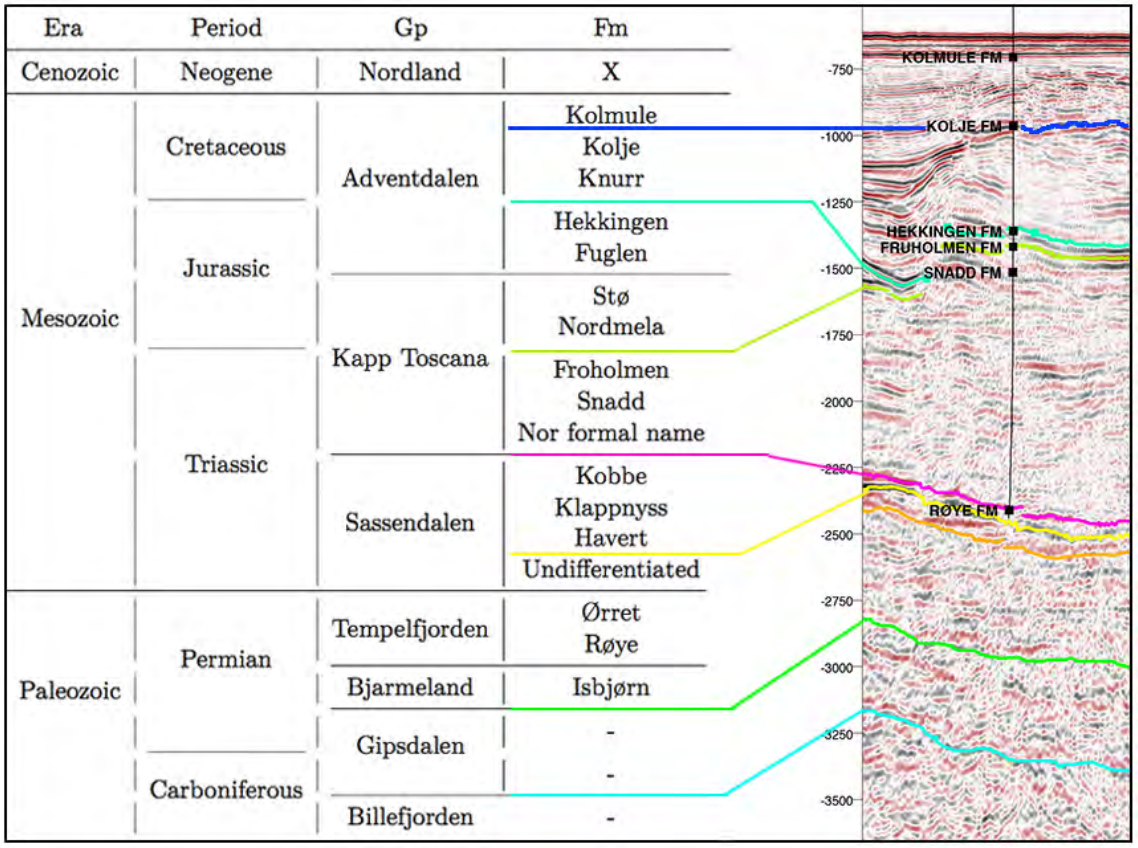

FIGURE 3.3: Well 7321/8-1 with its well tops and seismic tie. Note the colors used for horizon interpretation.

Petrel software by Schlumberger was used throughout the entire process of this thesis. In order to obtain the structural and geological configuration of the area a grid of 2D seismic lines was selected. The extent of the grid covers the main area of interest – Fingerdjupet Subbasin and its peripheral areas, western part of the Bjarmeland Platform and north-eastern part of the Bjørnøya Basin. The reason for this is to connect the interpretation of the basin to a regional scale. First, two selected reference horizons BCU (Base Cretaceous Unconformity) and Top Upper Triassic were outlined over the Fingerdjupet Subbasin and peripheral areas. Then several seismic lines avoiding areas with the presence of salt or areas of intensive faulting were selected to be able to link the interpretation of deeper reflectors in the Norvarg Dome with the study area.

Eight selected seismic key reflections were interpreted to represent the geological framework and describe the timing of tectonic movements and its effect on basin infill history. All reflections are described in detail below.

H8 - Aptian reflection was interpreted with the top Kolje Formation with the depth varying

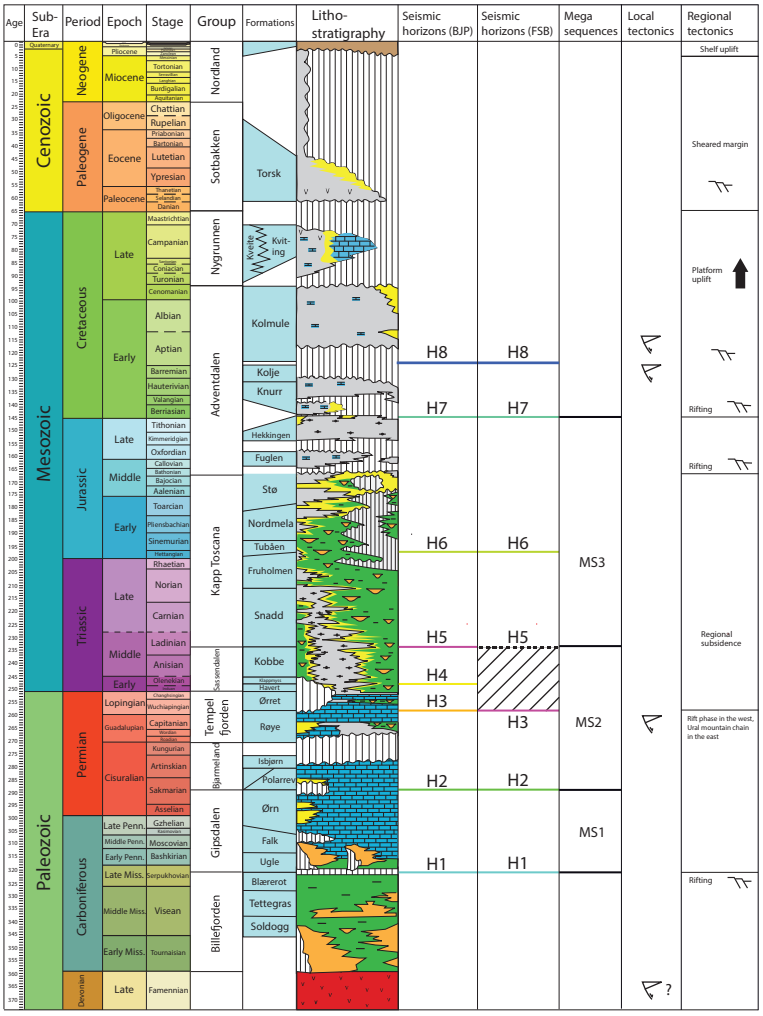

FIGURE 3.4: Lithostratigraphy of the western Barents Sea with major regional and locally observed tectonic events. Modified after Glørstad-Clark et al. (2010).

from ca. 1250 ms in TWT to the termination at the sea bottom in the eastern part of the Fingerdjupet Subbasin. The reflector is recognized by its strong amplitude, high frequency, high lateral continuity and negative reflection.

H7 - Base Cretaceous unconformity (BCU) reflection was correlated with the bottom of the Knurr Formation. The depth varies from approximately 2000 ms in TWT to the level of sea bottom where it truncates to the Quaternary sediments. The reflector is distinguished by its strong amplitude, high frequency, high lateral continuity and positive reflection. It represents a regional unconformity, which can be easily traced throughout the research area. Most of the faults interpreted in the Fingerdjupet Subbasin penetrate the BCU reflector.

H6 - Top Upper Triassic reflection was interpreted close to the top of the Fruholmen formation and the depth range is 2250 – 1000 ms in TWT. It is characterized by strong amplitude, high frequency, high to moderate lateral continuity and positive reflection. The reflector serves as the uppermost boundary of the thick Upper Triassic unit. It is worth mentioning that the reflector in some areas is very close to BCU reflector and the distance might be smaller than the distance of separability or even detectability.

H5 - Middle Triassic reflector is characterized by the strong-medium amplitude, medium frequency, high-medium lateral continuity, positive reflection and was tied with the top of the Kobbe Formation. However, in the Fingerdjupet Subbasin area the reflector coincides with the top of the Røye Formation, thus indicating absence of the unit from Late Middle Triassic to Late Permian in the area of interest, or this unit might be below the seismic resolution and could represent formation of 36 m in thickness named 'undifferentiated' in well 7321/8-1 (Table 3.1). The depth varies from approximately 3500 ms to 1750 ms in TWT. The reflection serves as the topmost boundary where prograding Upper Triassic clinoforms downlap onto.

H4 - Lower Triassic reflector was associated with the top of the Havert Formation which depth deviates from 3750 ms to 1650 ms in TWT. It is represented by moderate amplitude and frequency, moderate-low continuity with negative reflection.

H3 - Upper Permian reflector was correlated with the top of the Røye Formation and is represented by moderate amplitude, moderate frequency, moderate to low continuity and negative reflection. The depth of the reflector varies from nearly 3800 ms to 1700 ms in TWT and its moderate amplitude can be explained by the unsilicified clastic lithology. The reflection functions as the lowermost boundary where prograding Early Triassic units onlap onto and its distinctive feature is mound structures, interpreted as carbonate mounds in the Permian. However, these features are hardly detectable in the Fingerdjupet Subbasin because of the later tectonic movements.

H2 - lower Permian reflector is characterized by moderate-low amplitude, frequency, lateral continuity and negative reflection and was tied to the top of the Gipsdalen Group. The depth range is approximately 5000 - 2000 ms in TWT.

H1 - mid Carboniferous reflector was assumed to match with the top of the Billefjorden Group and is represented by medium-low amplitude and frequency, moderate lateral continuity, and negative reflector. The horizon was interpreted to be the first strong reflector caused by evaporates of the Billefjorden Group and overlain by nearly transparent reflections of carbonates in the Gipsdalen Group. Due to the great depth of the reflector, 5250 ms to 4000 ms in

TWT, the presence of peg leg multiples and low lateral continuity in the peripheral areas of the Fingerdjupet Subbasin interpretation might be doubtful.

Selected key seismic lines were printed and interpreted manually to better understand the complex faulting and infill of the basin. This process had proven to be a better option aiming detailed analysis than automatic tracking of surfaces in the Petrel software due to software limitations.

Six seismic key lines were selected to represent main observations obtained during the study of the Fingerdjupet Subbasin and will be presented in the subchapter 4.1. Selection is based on their location according to the wells, seismic resolution and representativeness of key observations.

Four time-structure maps were created for 4 levels: mid Carboniferous, early Permian, Middle Triassic and BCU to better understand the structural arrangement and faulting in the study area at different time intervals. Time-structure maps with interpreted faults will be discussed in more detail in the subchapter 4.2.

Interpreted succession from horizon H1 to H7 was subdivided into three megasequences and time-thickness maps were created to support the interpretation of sediment infill, and determine the varying thickness both vertically and horizontally. It will be presented in the subchapter 4.3.

Finally, fault maps were created for four levels introduced earlier: mid Carboniferous, early Permian, Middle Triassic and BCU to obtain a better understanding of the fault influence on the basin structural development and sediment infill directions. This will come up in the subchapter 4.4

Chapter 4

Results

In this chapter observations done in the study area will be presented. Six seismic key lines were selected to represent structural and stratigraphical framework of the Fingerdjupet Subbasin. Their selection was based on the location, orientation, quality and to illustrate identified features the best. The seismic succession interpreted from the Carboniferous until BCU was subdivided into three Megasequences. They were not segmented later to second order sequences due to the weak lateral continuity of seimic facies or their relatively small lateral extent.

4.1 Selected key lines

Key line 1

Line 1 (Fig. 4.1) is situated in the central northern part of the study area with a NW-SE orientation (approximately 14 km offset to the north from the Line 2 (Fig. 4.2). This section covers the north-easternmost corner of the Bjørnøya Basin, the Fingerdjupet Subbasin and westernmost part of the Bjarmeland Platform. Planar normal fault F13 and two listric normal faults F12 and F2 were defined as the main faults controlling the structural outline of the section. Based on the positioning of the main faults three main subareas were distinguished in the section: X – horst, C – half-graben, B – half-graben.

Subarea X is bounded by the faults F12 and F13 and displays a horst structure (Fig. 4.1). Interpreted horizons from H2 of Early Permian age to horizon H7 representing BCU are slightly dipping to SE and thickness in between remains constant. It has been interpreted that intrabasinal high is located further to the west in this section compared with the position of the Line 2 (Fig. 4.2). This horst is separated by a rotated fault block indexed C from the subarea B. The strong reflectors present below the intrabasinal high at ca. -3000 ms in TWT were interpreted as the possible apex of basement block described later more in detail with the Line 2. The position of the horst was assumed to be controlled by an eastward tilted basement block. It has been assumed that the orientation of the basement block tends to control the placing of the high.

Subarea C is restricted by the faults F12 and F2 and has the nature of a half-graben. As it can be seen (Fig. 4.1, subarea C), interpreted horizons from H3 of late Permian to H7, signifying BCU, do not reveal any particular dipping direction and lie nearly horizontally. Two different structural patterns of internal faulting, showing their own horst-graben topography, are present in the subarea at two different levels. One of these structural features penetrates the BCU horizon and another indicates faulting of late Permian age. The observed potential wedge-shape represented by strong reflections below the interpreted horizon H3 could support the late Permian faulting. In both fault patterns normal-drag structures are existent indicating time of faulting after sedimentation. The strong reflections dipping SE below the rotated half graben were interpreted to be the weakness zone formed between the basement block and overlying strata. This feature is described in more detail in the description of Line 2. Faults F12, F2 and internal faults of the subarea C could have detached at the weakness zone and continued to act as a low-angle listric normal faults.

Bounding faults for subarea B are F2 and F4, and reflectors within the subarea are dipping towards north-west (Fig. 4.1). However, the listric normal faults F3 and F4 can mark out additional subarea marked as B1 (Fig. 4.1, subarea B) in this section, which has a nature of a graben. Evidences of syn-sedimentary tectonics are present where wedge-shape geometry of a package of strata bounded by seismic reflections is observed right below the interpreted late Permian horizon H3. This package is thickening towards the F2 fault-plane, thus indicating that fault F2 was active during late Permian and reactivated during Late Jurassic – earliest Cretaceous and Aptian age. Later reactivation can be explained by normal-drag structures along the fault-plane of F2. In addition, strata wedges together with folding structures are present right above the BCU and Aptian horizons, thus signifying the activity of F2 at both stages. Subarea B2 has two separate fault patterns (Fig. 4.1), one initiating above Aptian and terminating below Upper Triassic, and another starting at the Middle Triassic and terminating within evaporites of Carboniferous age. Both fault patterns have horst-graben topography. The timing of internal structuring will be discussed in detail in the description of the Line 2.

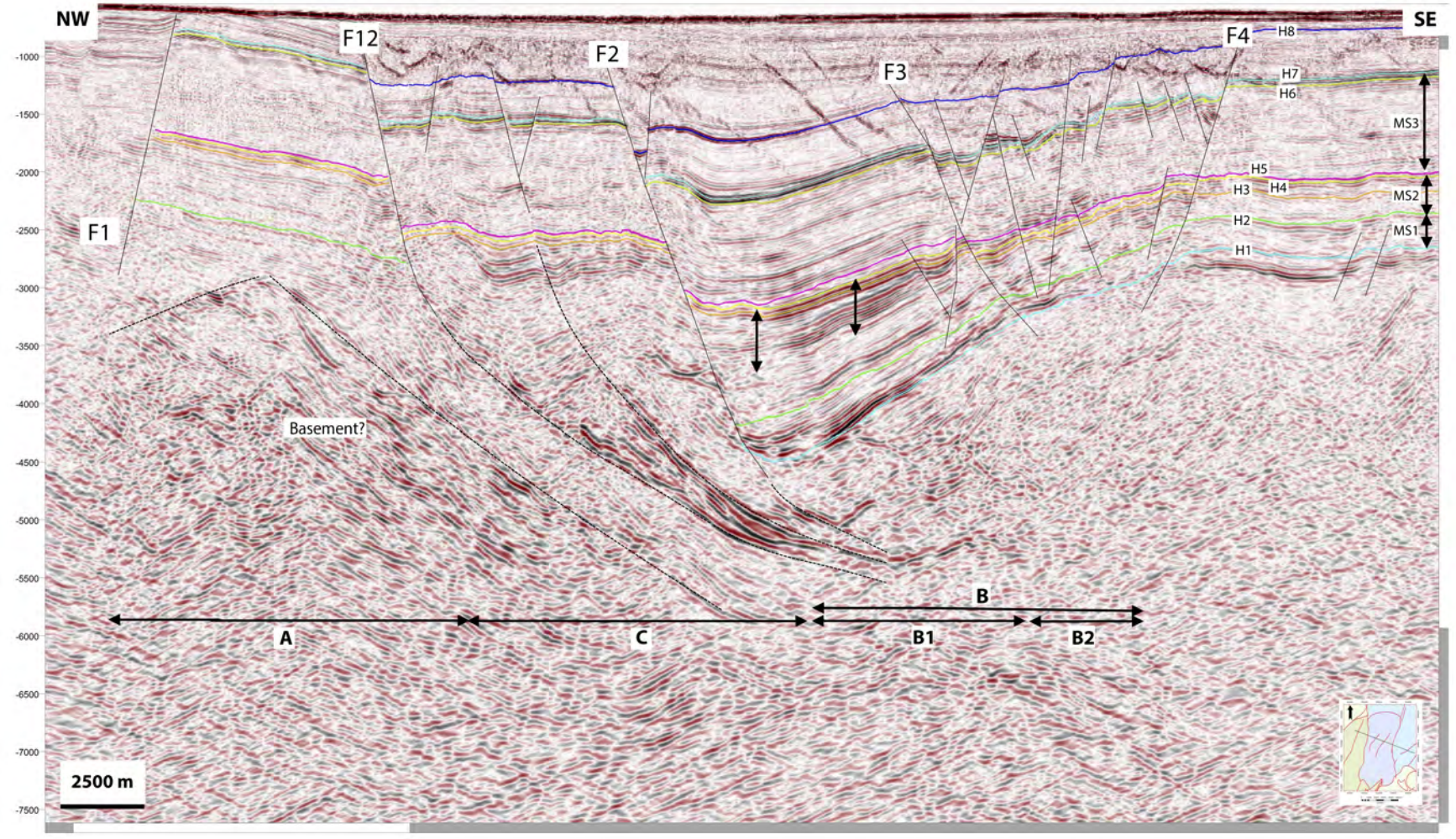

FIGURE 4.1: Seismic key line 1 with its location Fingerdjupet Subbasin in the lower right corner.

Key line 2

Line 2 is located in the central part of the study area with a NW-SE orientation (Fig. 4.2). It covers the easternmost part of the Bjørnøya Basin and the Fingerdjupet Subbasin. The planar normal fault F1, representing the Leirdjupet Fault Complex, and the listric normal fault F2 give the general structuring of the section. According to the faulting, the Fingerdjupet Subbasin (subarea B) is represented as a north-west dipping half-graben bounded by the intrabasinal high (subarea D) in the NW from the easternmost part of the Bjørnøya Basin (subarea A). The internal structuring in the Fingerdjupet Subbasin can be further subdivided into two separate subareas: B1 - rotated fault block and B2 – graben.

In the easternmost part of the Bjørnøya Basin (subarea A) two wedge-shaped sediment packages were detected at the level of horizon H8 representing Aptian and below the horizon H3 of late Permian age thickening towards the hanging-wall of the F1 (Fig. 4.2). It is hard to define the time when the F1 was active due to its termination just below the seabed and the erosion in Cretaceous and Cenozoic. However, the observed wedge-shape of the succession suggests that the fault was active both in late Permian and during Aptian rifting in the area. Moreover, normal-drag (interval from -2000 to -3000 ms in TWT) and folding structures at the level of horizon H7 are recognized along the fault-plane of the F1. Furthermore, potential reflection for H1 is marked with dashed line (Fig. 4.2) and indicate thickening unit between H1 and H2 thus suggesting active Carboniferous rifting along the F1 fault-plane.

An intrabasinal high is defined as a horst by the faults F1 and F2 (Fig. 4.2). Interpretation of horizons below the horizon H3 of late Permian level is tentative within the horst, because the seismic data becomes noisy and decrease in resolution. According to the interpreted BCU and late Permian horizons dip direction of the intrabasinal high towards south-east can be assumed. Moreover, discrete strong reflections representing potential wedge-shape in the lower part of the horst could support SE dip direction and late Permian faulting. Strong reflections at the level of ca. -4500 ms in TWT dipping to SE beneath the horst are interpreted to be basement reflectivity.

The Fingerdjupet Subbasin is confined by the main fault F2 and holds topography of rotated fault blocks (Fig. 4.2). Wedge-shape geometries of strata packages are present within the basin succession, showing thickening towards the hanging-walls of F2 and F3 at three levels: right below closely spaced horizons H3, H4 and H5, at horizon H7 and reflection of Aptian age. Moreover, normal-drag was observed along both faults F2 and F3. Clinoforms were interpreted to downlap the reflection right above the H5 and will be discussed more in detail in subchapter 4.3.3. It is hard to identify the timing when F2 and F3 were active, due to their termination

at the level of sea bottom and Cretaceous and Cenozoic erosion. The indications of syn-tectonic deposition described above suggest that the faults F2 and F3 were active during at least three episodes: the late Permian, Late Jurassic – earliest Cretaceous and Aptian times. The strong reflector below the subarea B (Fig. 4.2) is interpreted to represent a detachment zone where zone of weakness might have formed between the scarp of a basement block and the overlying layers, which allowed for the fault F2 to detach and continue along this boundary. This matches with the interpretation by Gudlaugsson et al. (1998) who stated that the Fingerdjupet Subbasin was formed in the Late Paleozoic as a half-graben in the hanging-wall of the basin-bounding listric normal fault. The internal structuring of the subbasin can be subdivided into two distinct subareas (Fig. 4.2): a rotated fault block bounded by the faults F2 and F3 and a graben outlined by the fault F3 and the listric normal fault F4. Timing of this internal structuring is hard to determine due to the absence of direct evidences of syn-tectonic strata features, but is assumed to be related to the Late Jurassic – earliest Cretaceous faulting. These faults appear to terminate right above the horizon H8 of Aptian age or below the seabed. It is worth mentioning that faults penetrating only the level of horizon H5 and not connected to other fault pattern could be related with the late Permian faulting or were active right after the deposition of the unit.

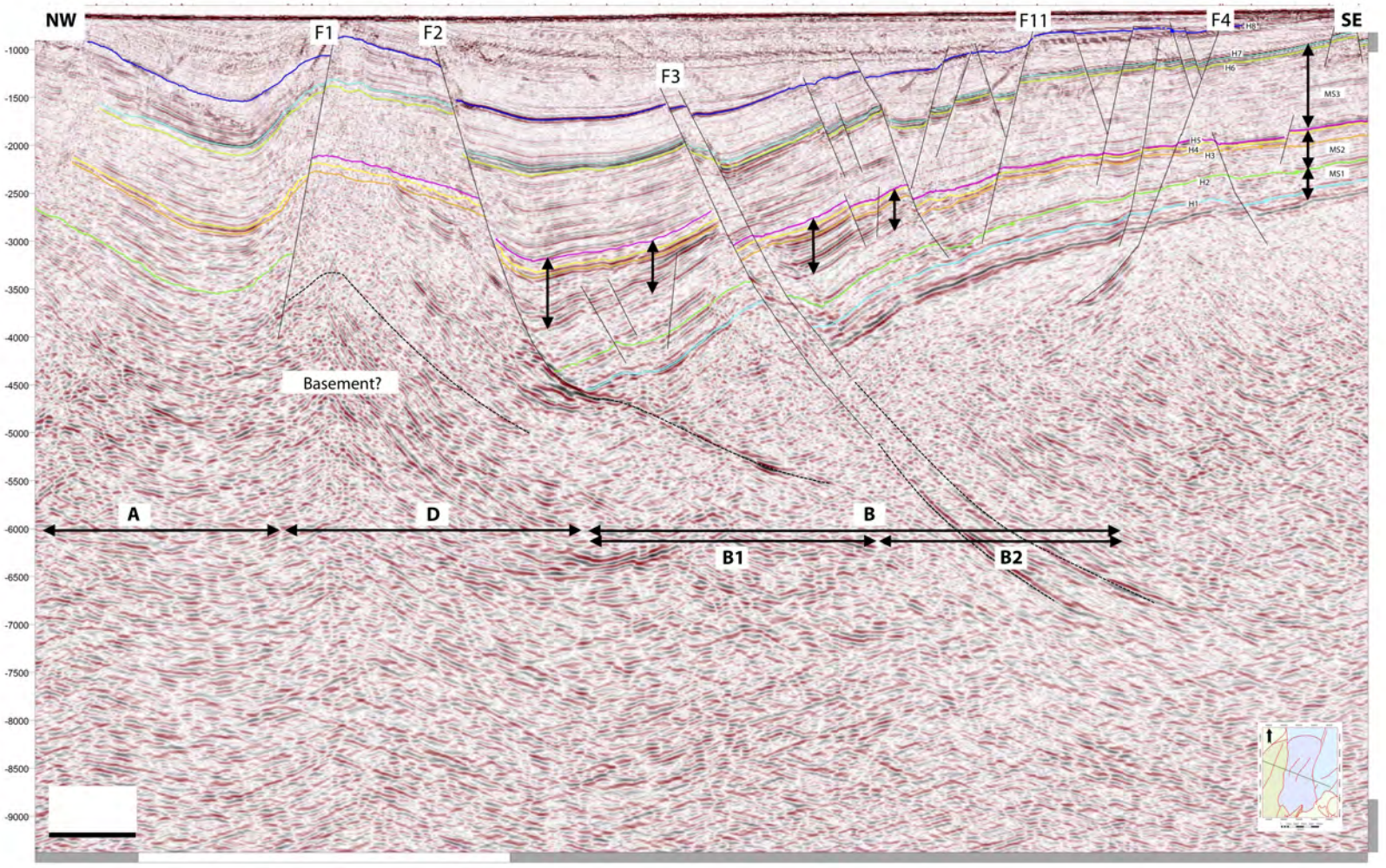

FIGURE 4.2: Seismic key line 2 with its location Fingerdjupet Subbasin in the lower right corner.

Key line 3

Line 3 is located in the central part of the study area and is oriented SW-NE direction, covering the easternmost part of the Bjørnøya Basin and the Fingerdjupet Subbasin (Fig. 4.3). The planar normal fault F1 (representing Leirdjupet Fault Complex) and listric normal fault F2 were outlined as the main faults, giving the structural setting and dividing section into three separate subareas: A – half-graben, D – horst and B – rotated fault block.

Subarea A is bounded by the main fault F1 (Fig. 4.3). Reflections are dipping NE towards the hanging-wall of the main fault. Thickness of the succession between interpreted horizons H2 and closely spaced horizons H3, H4 and H5 is gently increasing towards the fault-plane of F1, where wedge-shape structure is observed just below the horizon H3. In comparison, unit thickness between horizon H5 and H7 is constant within subarea A. Another wedge-shape thickening towards the hanging-wall of the fault F1 was interpreted at the level of horizon H8 of Aptian age. Normal-drag and folding structures were detected in subarea A along the fault-plane of F1.

Subarea D is defined by F1 and F2 and has the nature of a structural high (Fig. 4.3). Reflections in the deeper level of the horst tend to dip towards SW and NE, whereas at the level of interpreted horizons H6 and H8 the strata are dipping only to NE. As it was stated in the previous descriptions of the key lines (Key line 1, and 2), interpretation below the H3 horizon is uncertain due to noisy seismic data and decrease in seismic resolution. The graben has two different internal fault systems, one cutting the succession from H8 to H6 and another penetrating the interpreted succession from H5 to H1. Wedge-shape package situated right below the horizon H3 supports the idea of late Permian faulting. Strong reflections below the intrabasinal high might be caused by the basement block mentioned earlier in the descriptions of the key lines (Key Line 1, and 2). It is worth mentioning that reflections caused by interpreted basement block are much better pronounced in the Line 3 and indicate the geometry of asymmetric ridge.

Subarea B is defined by the fault F2 as the bounding fault of the large rotated fault block (Fig. 4.3). Layers are dipping towards the hanging-wall of the bounding fault. Thickness of the interpreted succession is relatively constant, only in the succession from H2 to H3 the thickness increases to the hanging-wall of F2 and wedge-shape is observed below the interpreted horizon H3 of late Permian age. Normal-drag structures were observed along the fault-plane of F2. Subarea B has three main internal fault patterns (Fig. 4.3): one set cutting only the level of horizons H5 or H8, another penetrating the succession from H7 until H2, and faults cutting the whole interpreted succession from H1 to H8. Strong reflections below the subarea B can be caused by Carboniferous evaporites or represent a weakness zone between the basement block

and overlying strata. Moreover, possible fault F9 penetrating basement block was marked with a dashed line.

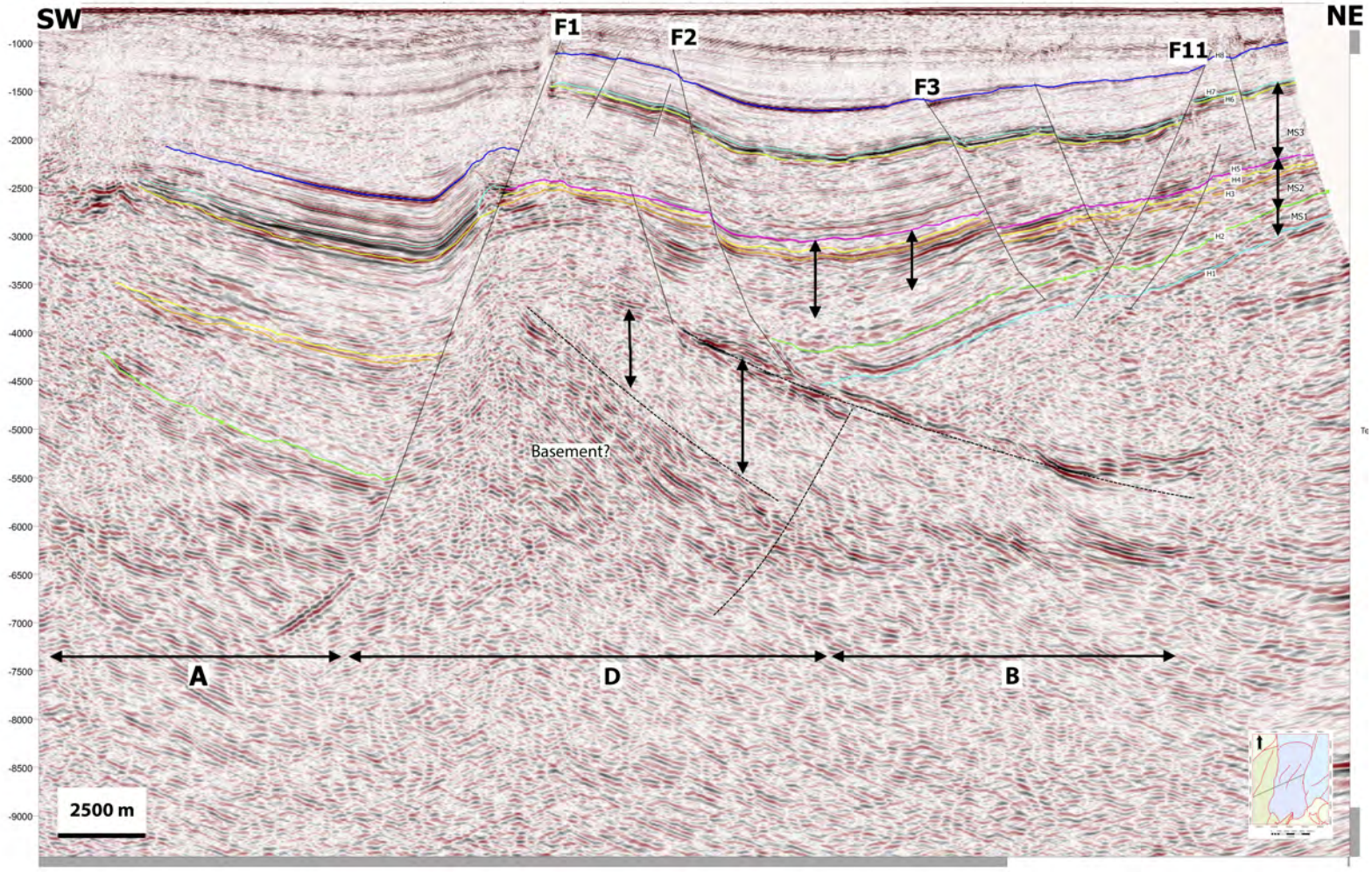

FIGURE 4.3: Seismic key line 3 with its location Fingerdjupet Subbasin in the lower right corner.

Key line 4

Line 4 is located in the southern part of the Fingerdjupet Subbasin with an orientation of NW-SE. The line transects the easternmost part of the Bjørnøya Basin and the Fingerdjupet Subbasin (Fig. 4.4). Four main faults are identified in the line. The planar normal fault F1 represents the Leirdjupet Fault Complex, faults F5 and F6 are both listric normal faults; and planar normal fault F7 subdividing subarea G; these four faults control the structural configuration of the Fingerdjupet Subbasin in this area. Based on the configuration of these main faults, Line 4 was divided into four distinct subareas: A – half-graben, G – half-graben, F – horst, E – half graben.

The subarea A is bounded by the F1, and the layers contained are dipping towards south-east (Fig. 4.4). It is clear that thickness increases towards the hanging-wall of the fault F1 in the unit from horizon H2 of early Permian age to horizon H3 of late Permian age; the wedge-shape structure is observed right below H3. The thickness of the succession above remains constant. Folding and normal-drag structures were observed along the fault-plane of F1. In addition, wedge-shape geometries are observed in the succession right above the horizon H7 and at the level of Aptian age. Moreover, potential wedge-shape can be observed in the deep part of subarea A, below interpreted horizon H2. Furthermore, possible reflection representing late Carboniferous (H1?) is marked with a dashed line (Fig. 4.4). As mentioned in previous key lines descriptions (Key line 2 and 3), it is hard to determine precisely the time of faulting of F1, due to the continuation of the fault up to the seabed and eroded Cretaceous and Cenozoic strata. However, detected wedge-shape structures suggest that F1 was active during at least four separate faulting episodes along the central part of the Fingerdjupet Subbasin.

The subarea G is confined by the faults F1 and F5 and reflections within the subarea are dipping towards SE (Fig. 4.4). The normal planar fault F7 is dividing the subarea into two distinct parts, each being rotated fault blocks. Normal-drag structures are present along the fault plane of F7 at the level of the BCU horizon H7. The thickness of the interpreted succession from H1 to H7 in the subarea seems to be fairly even. The wedge-shape packages of strata thicken towards F7 right above the horizon H7 of BCU age and the horizon H8 representing Aptian, and may thus indicate active faulting along the fault-plane of F7.

The horst-like feature in the subarea F is bounded by the faults F5 and F6 (Fig. 4.4). Layers within the subarea are dipping in NW direction. The subarea has two separate fault patterns revealing a horst-graben structural style within. There are indications of pre-Permian faulting in the lower part of this structural block, where present planar normal faults might become

detached listric normal faults in the deeper layers where strong reflectors with variable fault-plane are present (Fig. 4.4). Moreover, fault F9 outlined in the key line 3 penetrating the interpreted basement block is marked with dashed-line below the subarea G. In addition, wedge-shape thickening towards F9 is outlined. The timing of faulting along the fault-plane of F9 and possible syntectonic deposits will be discussed more in detail in Chapter **??**.

In the subarea E, structural configuration is bounded to the northwest by the fault F6, and layers are dipping in NW direction (Fig. 4.4). Wedge-shaped strata package is present above and below the interpreted horizon of mid Carboniferous age, thus indicating sedimentation during the time of faulting, (Carboniferous?). The succession from H2 until H7 has the same thickness within Line 4 in this subarea. Two sets of individual faults are observed, one penetrating interpreted Aptian horizon H8 and one reflectors of mid Carboniferous H1 and Early Permian H2 age. In the same subarea normal-drag structures can be observed along the fault plane of F6, at the level of interpreted Middle Triassic H5 horizon thus signifying that fault F6 was active during mid Carboniferous (?) and later reactivated. The subareas F and G were probably created during faulting in the Late Jurassic – earliest Cretaceous or Aptian age, as interpreted from the absence of direct faulting indicators in the deeper layers (Fig. 4.4). However, because of lack of evidences it is hard to resemble the previous structural setting in the section.

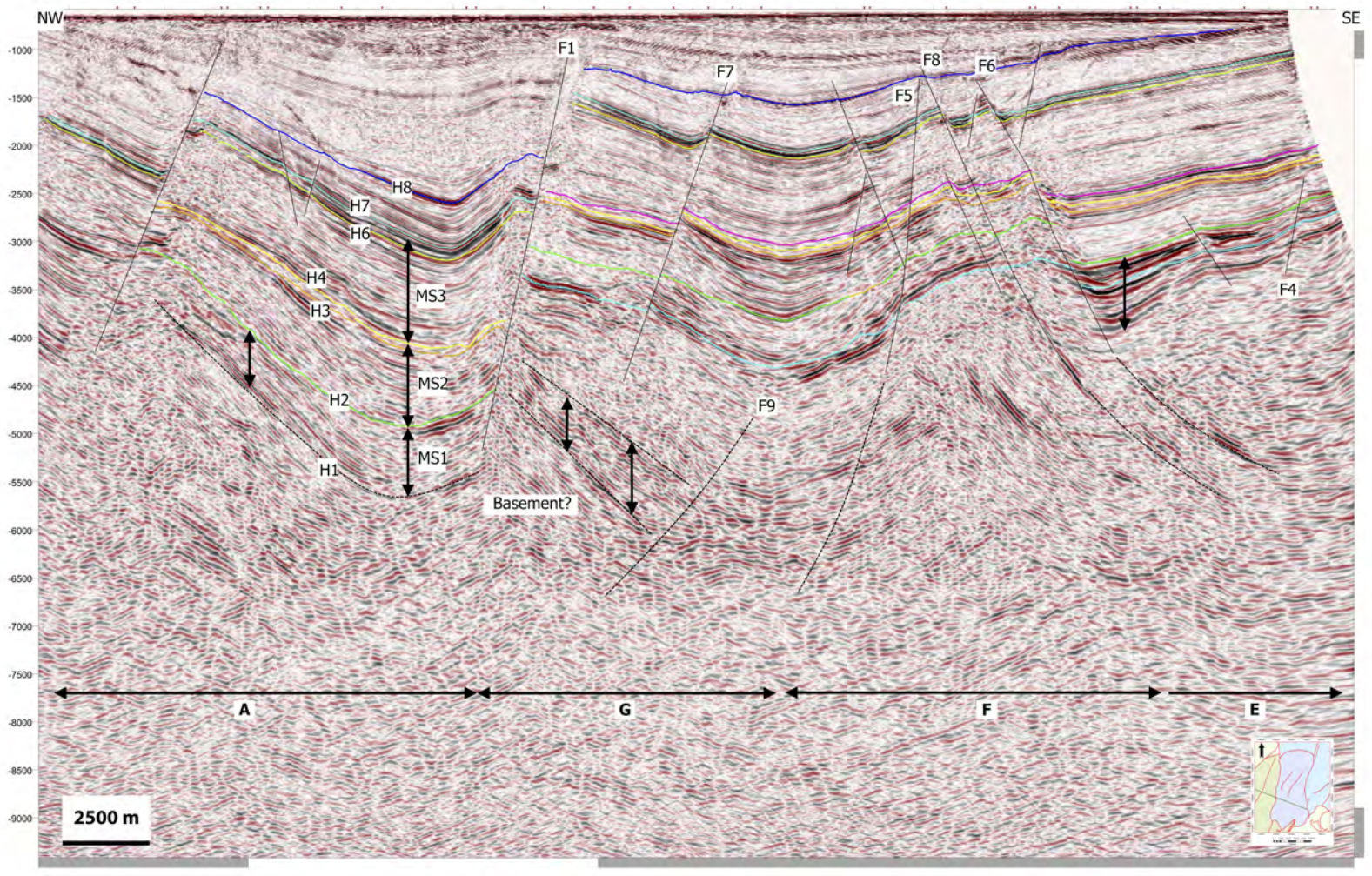

FIGURE 4.4: Seismic key line 4 with its location Fingerdjupet Subbasin in the lower right corner.

Key line 5

Line 5 is located in the southern part of the study area and is oriented NW-SE direction (Fig. 4.5). The line crosses the easternmost part of the Bjørnøya Basin and the Fingerdjupet Subbasin. Three main faults were outlined, together giving the structural setting of this section: F1 planar normal fault representing the Leirdjupet Fault Complex and F10 and F4 both being listric normal faults. According to the location of the main faults, the section can be subdivided into two distinct subareas: A – half-graben (easternmost part of the Bjørnoya Basin) and X – an area of several smaller rotated fault blocks.

Subarea A is bounded by the main fault F1 (Fig. 4.5). Layers are dipping towards SE. The thickness is fairly constant between the interpreted horizons H5 and H7 throughout the subarea, but in the lower unit, the succession confined by H2 and H3, shows thickness increasing towards the hanging-wall of the fault F1. Here a wedge-shape structure in the sediment package right below the H3 is observed. Another wedge-shaped strata geometry was interpreted right above the reflector H8 of Aptian age. Fault dragging is present along the fault-plane of F1 in the interpreted succession from H2 to H7. It can be assumed that F1 along the southern part of the Fingerdjupet Subbasin was active during two separate faulting events, as observed along the central part of the study area (see Fig. 4.1).

Subarea F is confined by the faults F1 and F4, and reflectors within the subarea are generally dipping towards NW, with an exception in the part close to the F1, where dip direction changes to SE (Fig. 4.5). Thickness of the interpreted succession is fairly constant throughout the subarea. However, wedge-shaped geometries in the succession were observed along the minor faults at the horizon H8 of Aptian age. An additional minor structural subarea can be outlined within subarea F (Fig. 4.5), bounded by the faults F4 and F6, which both are interpreted to be listric normal faults, thus giving this subarea the nature of a local graben. Potential wedge-shape sediment packages were interpreted to thicken towards the hanging-walls of the listric normal faults F6 and F9 at the level of the horizon H1. Thickness in stratigraphic unit with strong reflectors in the foot-walls of the faults F9 and F4 is greater than in the hanging-wall, thus suggesting that at the time of mid Carboniferous – early Permian (?) there might have been intrabasinal high, which during later faulting Late Jurassic – earliest Cretaceous (?) or Aptian (?) was transformed together with the whole section into a set of rotated fault blocks. Moreover, another potential wedge-shape is recognized thickening towards the fault-plane of F9 below the level of horizon H1.

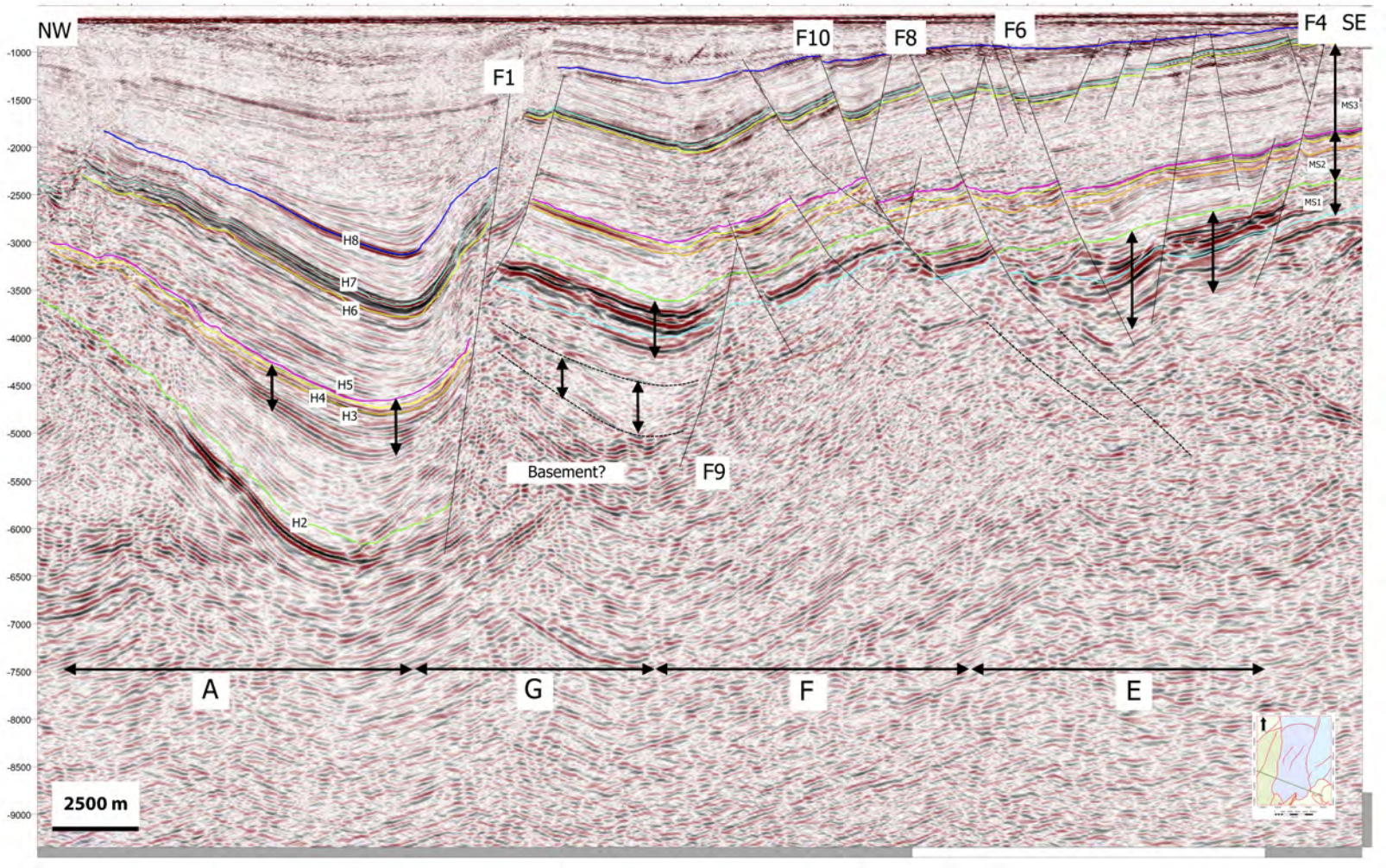

FIGURE 4.5: Seismic key line 5 with its location Fingerdjupet Subbasin in the lower right corner.

Key line 6

Line 6 is situated in the southern part of the study area and is oriented SW-NE (Fig. 4.6). The section crosses the easternmost part of the Bjørnøya Basin and the Fingerdjupet Subbasin. Two main planar normal faults, F1, F9 and listric normal fault F6 were interpreted to give the structural configuration of this part of the Fingerdjupet Subbasin. Based on fault interpretation three subareas were outlined: subarea G – half graben, F – structural high and E – rotated fault block.

Subarea G is defined by the faults F1 and F9 (Fig. 4.5). Reflections within the subarea are dipping to SW. In the succession defined from horizon H5 to horizon H7 at the depth of ca. -2750 ms in TWT prograding clinoforms can be observed, thus indicating the sediment transportation from NE or E, which will be discussed later in subchapter 4.3.3.

The faults F9 and F6 are bounding a horst with internal strata dipping to the SW (Fig. 4.5). Thicknesses between interpreted horizons seem to remain constant throughout the area. Few faults penetrate the whole succession between H1 to H8; some of the faults are associated with antithetic faults.

Fault F6 forms the main structural boundary towards the SW of the subarea E (Fig. 4.5). Layers within the subarea tend to dip towards SW, and the thickness of the strata units has a tendency to remain constant. However, potential wedge-shape geometry was observed at the level of H1 of mid Carboniferous age where it is thickening towards the hanging-wall of the F6. Three main fault patterns are present in the subarea: one set cutting only H8 and H7, penetrating the whole succession from H1 to H8, and one set starting above the H5 of Middle Triassic age and terminating right below the H2 of early Permian age.

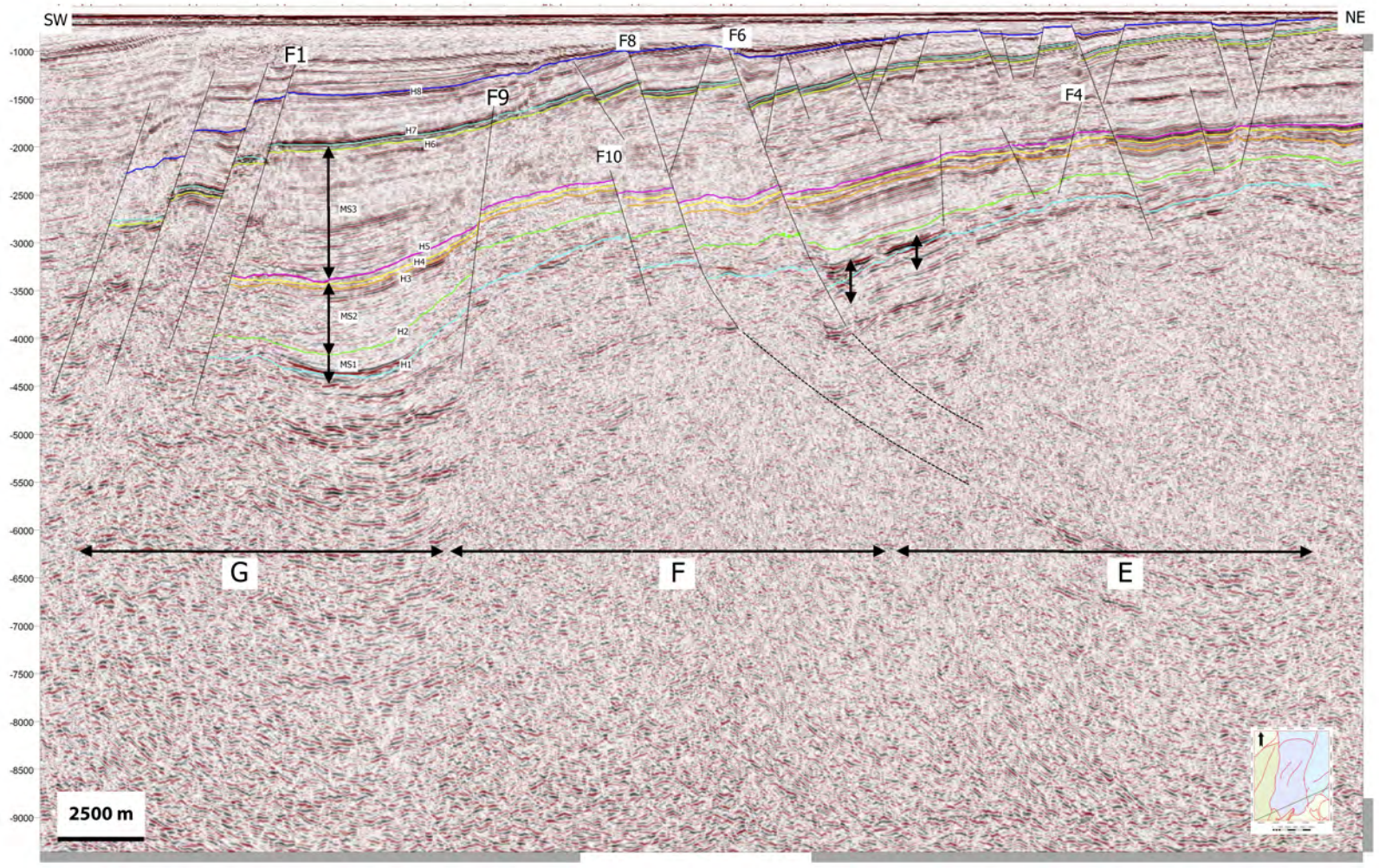

FIGURE 4.6: Seismic key line 6 with its location in the Fingerdjupet Subbasin in the lower right corner.

4.2 Time-structure maps

4.2.1 Mid Carboniferous

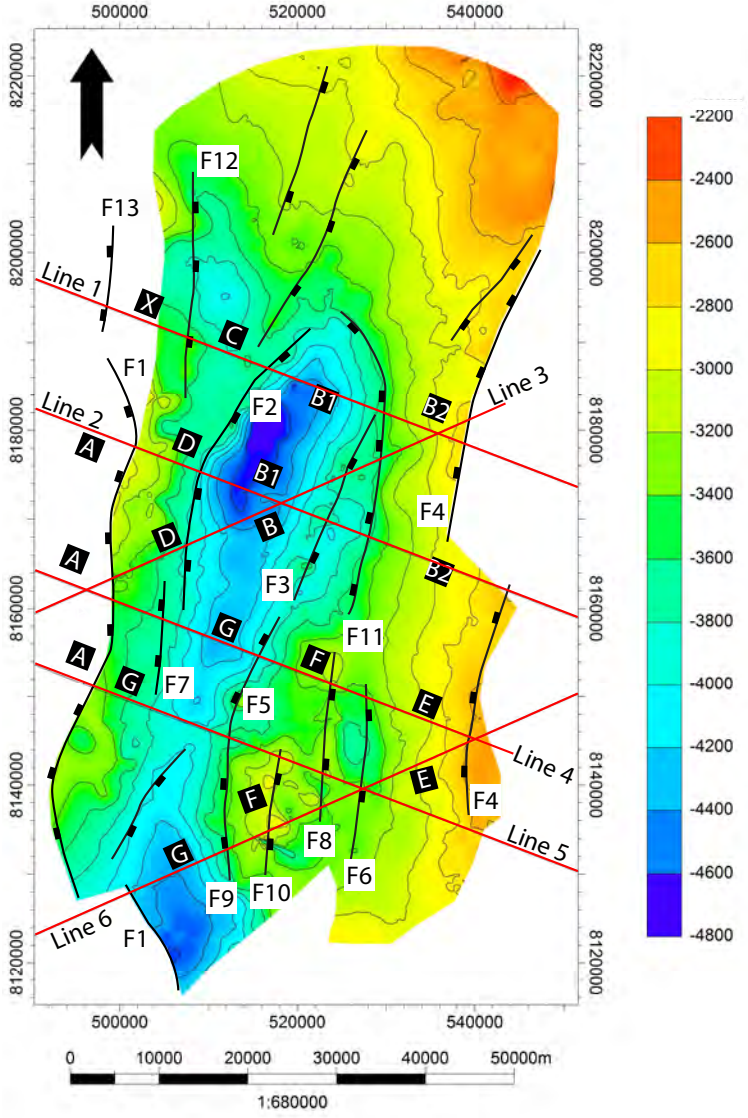

FIGURE 4.7: Time-structure map of interpreted mid Carboniferous level represented in ms in TWT. Note the key lines, main faults and structural elements indicated on the time-structure map.

Time-structure map of mid Carboniferous age with indicated main faults (Fig. 4.7) represent structural lineaments of three different directions NE-SW, NW-SE and N-S. Main normal faults F2 and F3 indicated in key lines (subchapter 4.1) are oriented NE-SW and define the half-graben structure dipping towards NW-W in the central part of the study area. Another half-graben to the south of the central half-graben is located and its dip direction is to the south or south-east. Local high trending NNE-SSW along the western margin of the subbasin and defined earlier in

key lines (subchapter 4.1) is not very well exposed. The reason for that could be uncertainties in the interpretation of mid Carboniferous horizon at the local high due to low seismic resolution and automatic interpolation of the software. Southern part of the Fingerdjupet Subbasin is mainly affected by N-S trending faults characterizing the area as a set of rotated fault blocks. Local graben structure is outlined in the southern part by N-S and NE-SW striking normal faults (Fig. 4.7). It is clear that mid Carboniferous horizon is shallowing gradually towards north and east, where the western part of the Bjarmeland Platform is located. Northern part of the study area is mainly affected by the NE-SW trending faults and has a nature of subplatform.

4.2.2 Early Permian

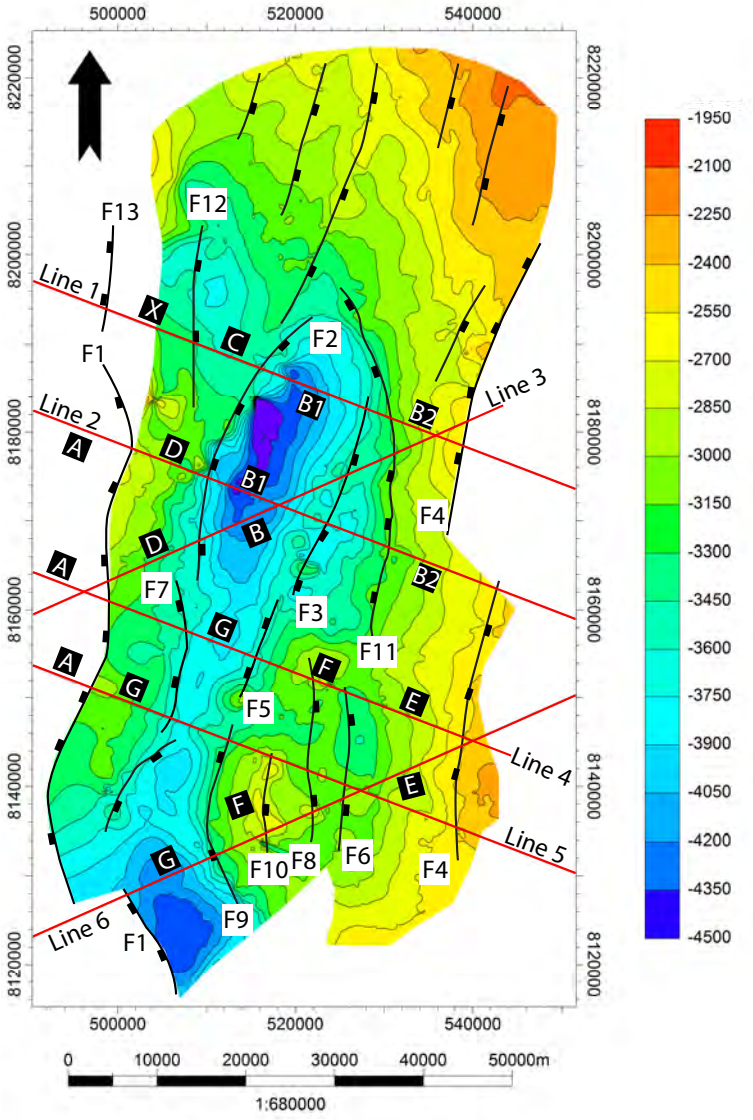

FIGURE 4.8: Time-structure map of interpreted early Permian level represented in ms in TWT. Note the key lines, main faults and structural elements indicated on the time-structure map.

Early Permian time-structure map (Fig. 4.8) represents almost the same features as indicated earlier for the time-structure map of mid Carboniferous age (Fig. 4.7). Main normal faults F2 and F3 maintain NE-SW direction and outline the half-graben structure in the central part of the study area. Noteworthy, second half-graben located to the south of the central reduces in extent compared with the mid Carboniferous time-structure map (Fig. 4.7). North-south trending normal faults define the eastern boundary of the local high that is prominent in the south-western part of the Fingerdjupet Subbasin. Southern part of the subbasin remains affected by N-S trending faults giving the nature of rotated fault blocks system and local graben

maintains its earlier position. In comparison with the mid Carboniferous time-structure map (Fig. 4.7), northern part in the early Permian becomes more affected by the NE-SW trending normal faults and has a nature of rotated fault block system. General depth trend is shallowing north and east towards western part of the Bjarmeland Platform.

4.2.3 Middle Triassic

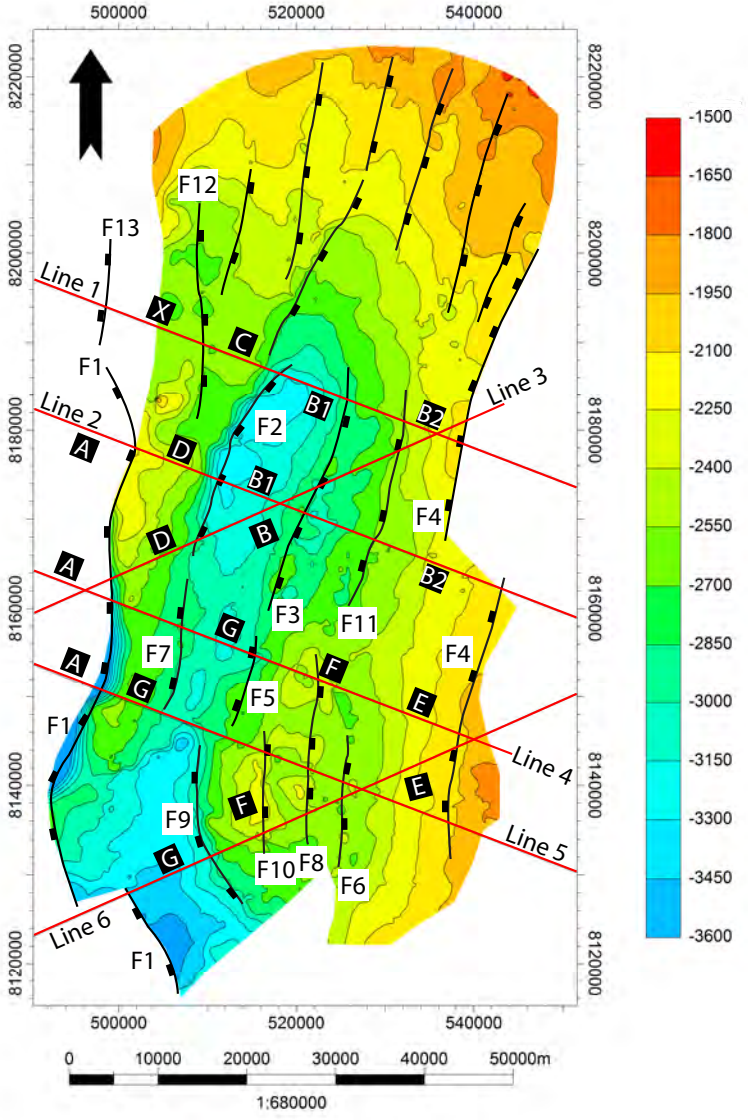

FIGURE 4.9: Time-structure map of interpreted early Permian level represented in ms in TWT. Note the key lines, main faults and structural elements indicated on the time-structure map.

Middle Triassic time-structure map represents earlier described structural trends of NE-SW and N-S. Main normal faults F2 and F3 preserve NE-SW orientation and marks sharp boundary between half-graben in the central part of the study and local high in the west (Fig. 4.9).

The placement and trend of the local high becomes more pronounced in the Middle Triassic time structure-map compared with earlier described maps of mid Carboniferous (Fig. 4.7) and (Fig. 4.8) early Permian age. Faults F4 and F11 are giving the internal structure of graben inside the half-graben defined by the main faults F2 and F3. Half-graben located to the south of the central half-graben reduces in extent and shifts slightly towards south. Small-scale half-graben evolves in the north-western corner of the Fingerdjupet Subbasin. In the south-western part abrupt decrease in the TWT is observed indicating the Leirdjupet Fault Complex dipping towards west and separating local high from deep Bjørnøya Basin (Fig. 4.9). Intensity of faulting penetrating the level of the Middle Triassic increases even more in the northern part of the study and preserves NE-SW trend. All the faults in the northern area are dipping towards SE and represents complex of rotated fault blocks. Southern part retains N-S trending faults and general configuration of rotated fault blocks. Local graben present in the level of mid Carboniferous (Fig. 4.7) and early Permian (Fig. 4.8) is not very well exposed in the time-thickness map of Middle Triassic. The surface of Middle Triassic contains gradual shallowing to the east towards the Bjarmeland Platform and north where it represents subplatform.

4.2.4 BCU

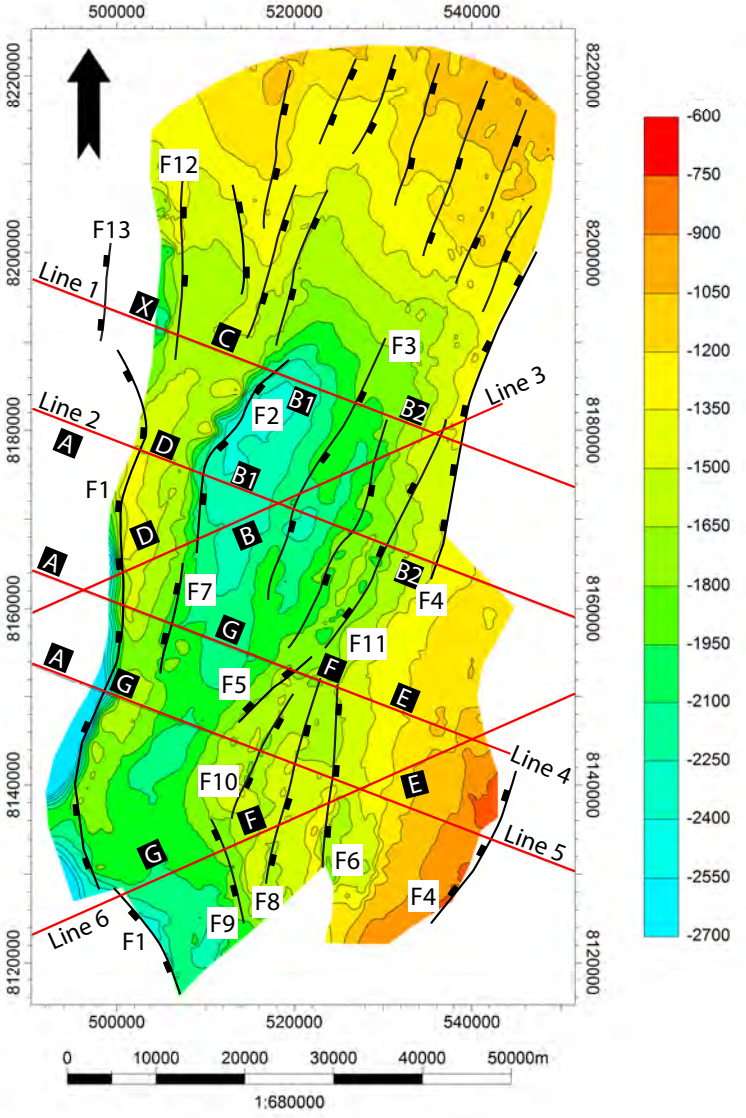

FIGURE 4.10: Time-structure map of interpreted BCU level represented in ms in TWT. Note the key lines, main faults and structural elements indicated on the time-structure map.

In the time-structure map of BCU level the same structural setting as described earlier is remained (Fig. 4.10). Main normal faults F2 and F3 defining the half-graben are present however, their orientation rotates slightly towards east. Their extent is also increasing both in the direction of north-east and south-west. The same shift in the orientation can be observed in the southern part where faulting trend from mid Carboniferous until Middle Triassic levels was N-S (Fig. 4.7, 4.8, 4.9) and in BCU it shifted to the east and local high is not definite anymore. The intensity of faulting in the northern part of the Fingerdjupet Subbasin increases even more with faults trending NE-SW and dipping towards south-east thus representing complex of rotated

fault blocks, however the rotated fault block is less prominent. The extent of the half-graben rotated to the south of the central graben decreases even more. The local high allocated in the western part of the study area becomes more pronounced and it extends towards south. As mentioned in the description of the Middle Triassic time-structure map (subchapter 4.2.3), there is sharp decrease in TWT in the south-western part of the study and its extent shifts slightly towards east hence proving the dip direction of the Leirdjupet Fault Complex.

4.3 Time-thickness maps

4.3.1 Megasequence 1

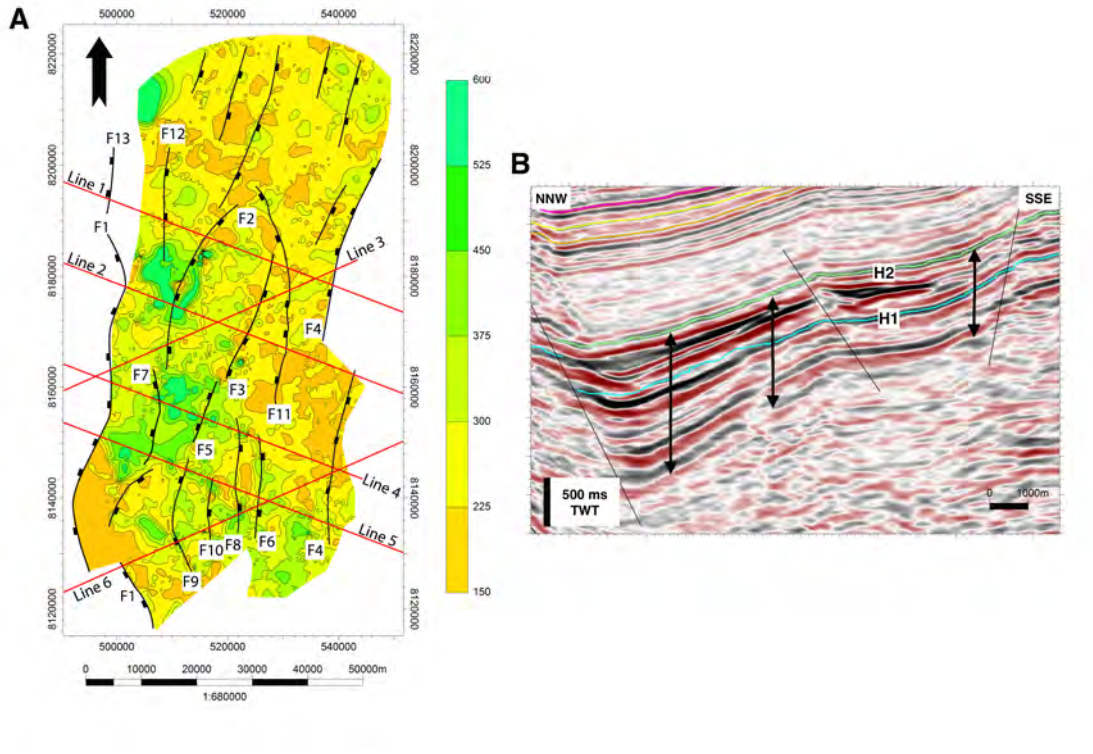

FIGURE 4.11: Time-thickness map of Megasequence 1 between mid Carboniferous and early Permian horizons, thickness is represented in ms in TWT; B - wedge-shape in the southern part of the Fingerdjupet Subbasin thicknening towards fault-plane of F6. Note the key lines, main faults and structural elements indicated on the time-thickness map.

Description

The lower boundary of Megasequence 1 is defined by interpreted horizon H1 assumed to be of mid Carboniferous age and the upper limit by horizon H2 of early Permian age (Fig. 4.11 A). For the detailed information how the age of the interpreted horizons was established see

Chapter 3. In the northern and central parts of the study area Megasequence 1 is dipping to W-NW towards the Bjørnøya Basin and shallowing eastwards to the western part of the Bjarmeland Platform. At the local high situated in the south-western part of the Fingerdjupet Subbasin dip direction changes to S-SW.

The thickness observed from the time-thickness map (Fig. 4.11 A) appears to vary from 150 to 500 ms in TWT throughout most of the study area and reaching up to 675 ms in TWT in the central west and south of the Fingerdjupet Subbasin.

Subparallel reflector pattern is dominant throughout the MS1, with local divergent pattern occurrences in the southern part of the Fingerdjupet Subbasin where a growth-fault is detected and strong seismic reflections reveal wedge-shape geometry of the succession, thickening towards the hanging wall of the main fault F6 (Fig. 4.11 B). Bottom part of the megasequence is characterized by strong amplitude reflectors, whereas its upper part contains moderate to low amplitude reflectors.

The level of faulting cutting MS1 is the lowest compared with other outlined megasequences. Several fault patterns were observed cutting the Megasequence 1: main faults penetrating the whole interpreted succession from horizon H1 of assumed mid Carboniferous age up to horizon H8 correlated to represent Aptian; faults only cutting MS1 and not being connected with the main fault pattern; and faults terminating right below the upper limit of the MS1. Dragging structures are recognized along the fault plane of the main faults throughout the study area.

Interpretation

Dipping of Megasequence 1 towards W-NW was caused by the extensional regime in the area, which acted along the main faults F6 and F9 cutting all interpreted succession from H1 of mid Carboniferous age to H8 representing Aptian during the late Permian and from Late Jurassic to Early Cretaceous. Before, main tilting was executed with reference on comparatively varying thickness in time-thickness map (Fig. 4.11 A), it can be concluded that depositional conditions during the sedimentation of MS1 in the Fingerdjupet Subbasin was close to the platform environment, when underlying structural relief with varying thickness was gradually infilled with the possible presence of differential subsidence. Growth-faults observed in the southern part of the study area (Fig. 4.11 B) indicate that faulting was present during the deposition of MS1. It is worth mentioning that the wedge-shape structures pass into the layers below the lower boundary of MS1 (Fig. 4.11 B) thus specifying that faults were active before the deposition of megasequence. The fault pattern terminating right below the upper boundary of the megasequence 1 might indicate that rocks in the upper part of MS1 (interbedding dolomites and evaporates) acted more ductile than the overlying rocks (massive limestones) or that the

stress regime ceased at the depth of termination. Change in the dip direction of the reflections at the local high present in the south-western part of the Fingerdjupet Subbasin (Fig. 4.5) and dragging structures along the bounding fault specifies formation of the local high after the deposition of the Megasequence 1. However, seismic reflections in the local high are very dim (Fig. 4.2, subarea D), especially at the depth of MS1 and the dip direction might be debatable. It is worth mentioning that the differences in time-thickness can be apparent, being related to uncertainties in the interpretation of H1 due to the great depth and seismic amplitude loss, no seismic to well tie and only assumed real age. High amplitude reflectors in the lower part of the Megasequence 1 and nearly transparent seismic signature in the upper part might have been caused by the succession passing from cyclical dolomites and evaporates to massive limestones and their different seismic velocities (Fig. 4.11 B). For the detailed explanation see Chapter 2. Subparallel reflection pattern, which is dominating in the MS1 throughout the Fingerdjupet Subbasin indicates that at the time when Megasequence 1 was deposited regional subsidence was present in the area.

4.3.2 Megasequence 2

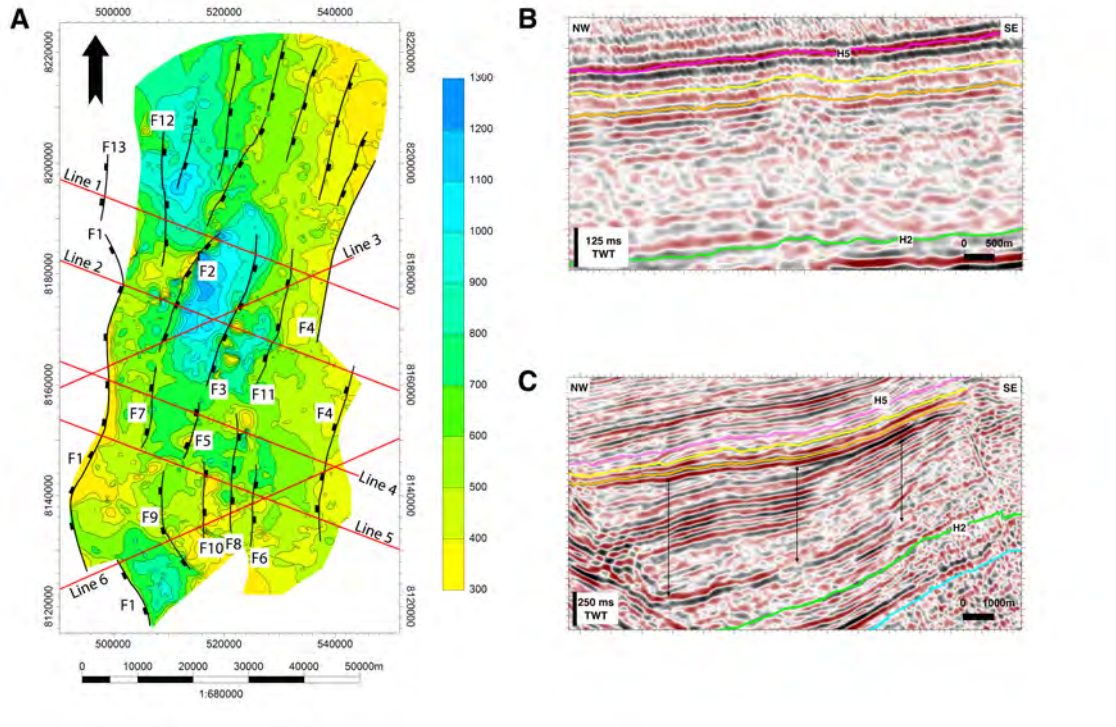

FIGURE 4.12: A - Time-thickness map of Megasequence 2 between early Permian and Middle Triassic horizons, thickness is represented in ms in TWT; B - close up line representing parallel reflection pattern; C - wedge-shape in the central part of the Fingerdjupet Subbasin thicknening towards fault-plane of F2. Note the key lines, main faults and structural elements indicated on the time-thickness map.

Description

Megasequence 2 was interpreted to be stratigraphically located between traced horizon H2 of early Permian age and horizon H5 of Mid Triassic age. As MS1, this megasequence is dippining to W-NW, towards the Bjørnøya Basin and shallowing eastwards to the western part of the Bjarmeland Platform. Dip direction changes to S-SW at the local high in the southern part of the study area.

Values in the time-thickness map (Fig. 4.12 A) vary greatly from 300 to 1250 ms in TWT over the Fingerdjupet Subbasin and reach the greatest thickness in the central and northwestern parts. In the areas of maximum thickness MS2 tends to pinch out towards the western side of the Bjarmeland Platform.

Megasequence 2 is highly faulted and several fault patterns were detected penetrating the MS2: main faults cutting the entire interpreted succession from the H1 of predicted mid Carboniferous age and H7 representing BCU; individual faults present only within this megasequence; and faults which are connected with the fault pattern in the MS3 and terminates right below the lower boundary of the Megasequence 2. Dragging structures are present throughout the entire MS2 in most of the Fingerdjupet Subbasin. In the central and southern parts of the study area, Megasequence 2 can be subdivided into two parts. Lower part is defined by the subparallel moderate to low amplitude reflection pattern (Fig. 4.12 B); whereas in the upper part the reflection characteristic shifts to divergent strong amplitude pattern and wedge-shapes thickening towards the hanging-wall of the main faults are observed in MS2 (Fig. 4.12 C). In the other parts of the study area MS2 contains the same seismic facies as the defined lower part of the megasequence in the central area of the Fingerdjupet Subbasin.

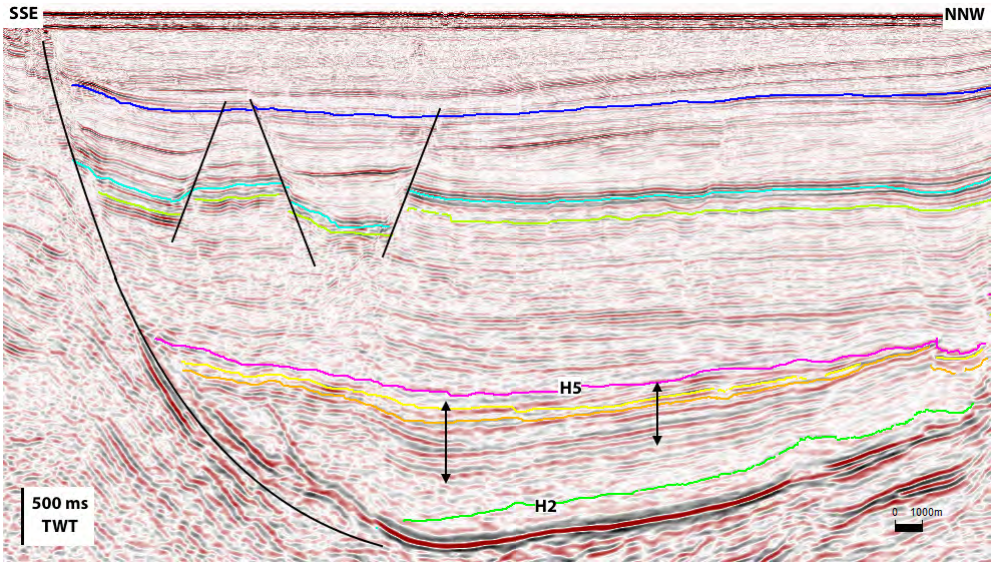

FIGURE 4.13: Wedge shape observed in the southern part of the Fingerdjupet Subbasin below horizon H3 of early Permian age.

Interpretation

The same dip direction as in the MS1 have been caused by the same extensional regime that acted on the same main faults F6 and F9 penetrating the succession from H1 of predicted mid Carboniferous age to H8 indicating Aptian, which were active during the late Permian and from Late Jurassic to Early Cretaceous. Thinning of the sequence in the central part of the study area towards western side of the Bjarmeland Platform indicate that during deposition, greater accommodation space existed in the western and north-western side of the Fingerdjupet Subbasin (Fig. 4.12 A).

Observed fault-growth in the central and southern parts of the study area specifies that faults F2 and F3 and The Bjørnøyrenna Fault Complex were active during the deposition of the Megasequence 2 (Fig. 4.12 C) and (Fig. 4.13). It is difficult to comment the timing of other fault patterns present in the MS2 due to the lack of direct evidences of syntectonics. Nonetheless, the fault pattern that initiates right above to upper boundary of Megasequence 2 might have acted right after the deposition of the MS2. The fact that this fault pattern does not penetrate MS1 might indicate stress regime of short duration or lithological affect where siliciclastic sediments composing the upper part of MS2 act more brittle than the lower part of MS2 where carbonates are present and during the faulting act more as a decollement zone. It is clear from time-thickness map (Fig. 4.12 A) that depocenter moved towards the central and north-western part of the study area in the MS2 thus indicating that at a time greater accommodation space was created.

Subparallel reflection pattern in the lower part of the megasequence (Fig. 4.12 B) suggests its sedimentation during the ongoing subsidence in the area. The reason for its low amplitude reflectors could be caused by the lithology and different seismic velocities, where Permian limestones having dim reflections are overlying evaporites, which age is expected to be of Carboniferous and produce strong seismic reflections. Factors leading to a shift from low to strong amplitude reflectors in the upper part of the MS2 could be due the change in the lithology from Permian carbonates to Early Triassic siliciclastic sediments and their diverse acoustic impedance.

4.3.3 Megasequence 3

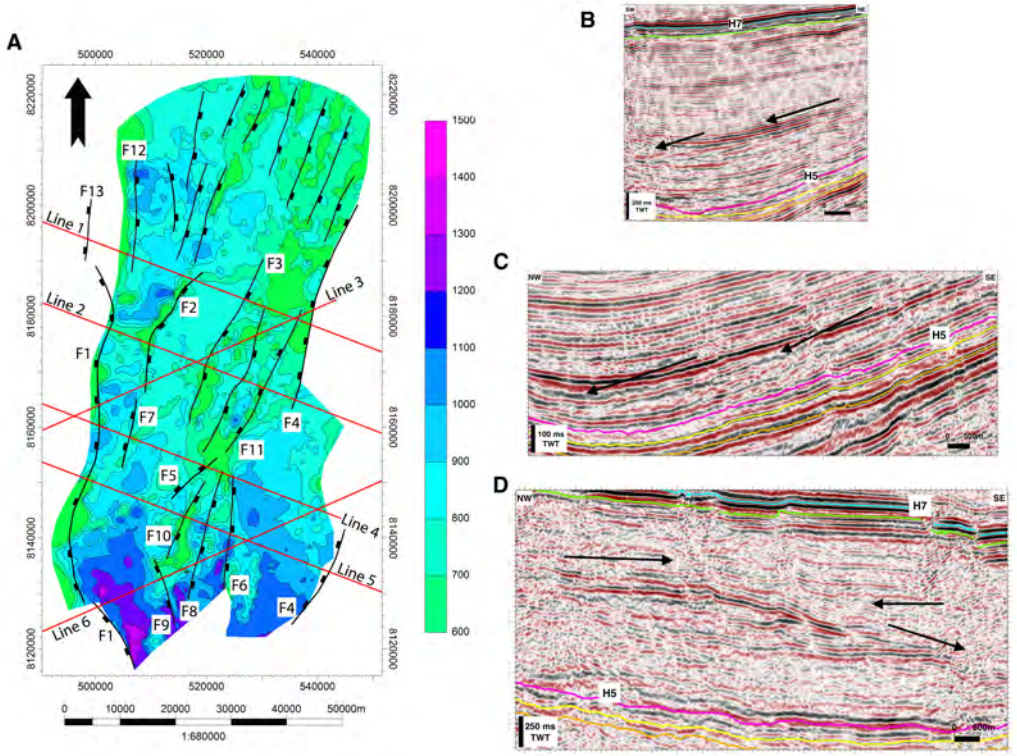

FIGURE 4.14: A - Time-thickness map of Megasequence 3 between Middle Triassic and BCU horizons, thickness is represented in ms in TWT; B - SW prograding packages in the middle part of the MS3; C - NW prograding units and downlaping interpreted maximum flooding surface; D - sedimentary packages prograding towards SE in the northern part of the Fingerdjupet Subbasin. Note the key lines, main faults and structural elements indicated on the time-thickness map.

Description

Megasequence 3 was distinguished between interpreted horizon H5 of Middle Triassic age and horizon H6 representing Top Triassic age. Like MS1 and MS2, this megasequence is generally dipping in N-NW direction towards the Bjørnøya Basin and shallowing to the east, where western side of the Bjarmeland Platform is located. The thickness of this megasequence based on the time-thickness map (Fig. 4.14 A) varies from 600 to 1450 ms in TWT and two zones of greater thickness can be defined: one located in the southern part of the study area, where the thickness is greatest; and another situated in the north-western part.

MS3 is moderately faulted with numerous fault patterns present: main faults penetrating the whole interpreted succession from H1 of assumed mid Carboniferous age to H8 indicating Aptian; faults only present in Megasequence 3; fault pattern that is terminating right below the lower boundary of MS2 and its antithetic faults; and fault pattern that starts immediately

above the lower boundary of MS3 and terminates in MS2. No fault-growth was determined in Megasequence 3, only fault-dragging structures along the fault-plane of F2 exist in the northern and central parts of the study area (Fig. 4.1). It can be seen at the thickness map (Fig. 4.14 A), lineaments orientated NNE-SSW are densely located in the northern part of the Fingerdjupet Subbasin and extends towards south. In comparison with the time-structure maps of BCU (Fig. 4.10) and Middle Triassic (Fig. 4.9) becomes clear that the orientation of the lineaments is identical to the orientation of faults.

In the central and northern parts of the Fingerdjupet Subbasin, MS3 can be subdivided in two distinct units. The lower unit is of approximately 200 ms in TWT in thickness and is characterized by prograding strong amplitude clinoforms from E-SE to N-NW (Fig. 4.14 C). The clinoforms downlap onto the reflector located above the interpreted horizon H3 of Middle Triassic age. Both in the Fingerdjupet Subbasin and the Bjarmeland Platform clinoforms have sigmoidal foreset geometry with slope angle being ca. 1° and nearly similar. Clinoforms in the study area have better pronounced topset and bottom set and stronger seismic reflections (Fig. 4.14 B and C). The upper unit of the MS3 is of ca. 800 ms in TWT in thickness and is characterized by subparallel moderate amplitude seismic reflection pattern. However, in the northern part of the Fingerdjupet Subbasin individual clinoforms prograding from NW to SE and having sigmoidal foreset geometry with angle approximately 2° were observed (Fig. 4.14 D). Topset and bottom set are rather prominent.

Interpretation

The W-NW dip direction of Megasequence 3 is assumed to be the result of the same extensional regime which acted on the same faults F2 and F3 as previously described in MS2 and MS1 (subchapters 4.3.1 and 4.3.2).

From the time-thickness map (Fig. 4.14 A) it is clear that the depocenter that existed at the central part of the Fingerdjupet Subbasin during deposition of the MS2 (Fig. 4.12 A) vanished during formation of the MS3 and the depocenter in the north-western part of the area increased in its lateral extent compared with its extent in Megasequence 2. The disappearance of the depocenter in the central part of the study area indicates changes in the intensity of the local subsidence, which was slower or absent in the central part during the deposition of MS3. The local subsidence in the north-western part of the Fingerdjupet Subbasin remained the same or slightly increased, which allowed for the depocenter to increase in the extent. Moreover, a new depocenter was established in the south, close to the north-western margin or slope of the Loppa High, thus indicating that greater accommodation space had been created here at the time of deposition of MS3.

Absence of wedge-shape structures gives no direct timing of faulting during the deposition of MS3. Fault patterns described in the description part are the result of later faulting that was present in the study area. Presence of fault-dragging in the MS3 over the Fingerdjupet Subbasin tells that faulting occurred after the strata were deposited. The lineaments present in the time-thickness map (Fig. 4.14 A) might be the result of faulting after the deposition of Megasequence 3 and could be the direct indicator that extensional forces were oriented NW-SE direction.

According to the separation into two units at the central and northern parts of the study it seems that Megasequence 3 experienced two different episodes of deposition. Lower unit with clinoforms (Fig. 4.14 B and C) had formed by sediment progradation from east and south-east and gradually filling in a distal part of the basin with relatively low sea level. Sudden change to the upper unit of MS3 where subparallel reflection pattern and thickness is much greater than in the lower unit could indicate change in the depositional environment from progradational to aggradational sedimentation from suspension or the onset of regional subsidence when accommodation space was constantly created. In addition, individual clinoforms (Fig. 4.14 D) coming from west or nort-west might indicate sediment transportation from local source areas, which developed during the time when the basin was subsiding.

4.4 Fault interpretation

4.4.1 Bounding faults

The Leirdjupet Fault Complex

Description

The Leirdjupet Fault Complex is separating the Fingerdjupet Subbasin in its western part from the deeper Bjørnøya Basin. According to Gabrielsen et al. (1990) structural style of the fault complex changes alongside the strike. Therefore it can be subdivided into three distinct segments (Fig. 4.15). The fault system is comprised of one normal fault in the northern segment (Fig. 4.15, A) and is dominated by a horst-graben topography. In the central segment (Fig. 4.15, B), the fault complex is characterized by one normal fault and large throw. While in the southern segment (Fig. 4.15, C) it splits into several normal faults, which were rotated. Polarity of the faulting is interpreted as synthetic and the fault-plane dips westwards. Strike of the fault complex is orientated in N-S direction in the southern part, when in the central part it shifts towards NW-SE. The throw of the fault complex is much greater in the south and ceases towards the north (Fig. 4.15). Wedge-shape strata geometries were observed right below the

interpreted horizon H3 of the late Permian age, at the levels of horizons H7 and H8 representing BCU and Aptian age respectively. Moreover, potential wedge-shape was interpreted to thicken towards the main fault-plane between possible horizon H1 of mid Carboniferous age and horizon H2 representing early Permian. The Leirdjupet Fault Complex contains normal-drag indications along the main fault-plane throughout the Fingerdjupet Subbasin and folding structures at the BCU and Aptian levels.

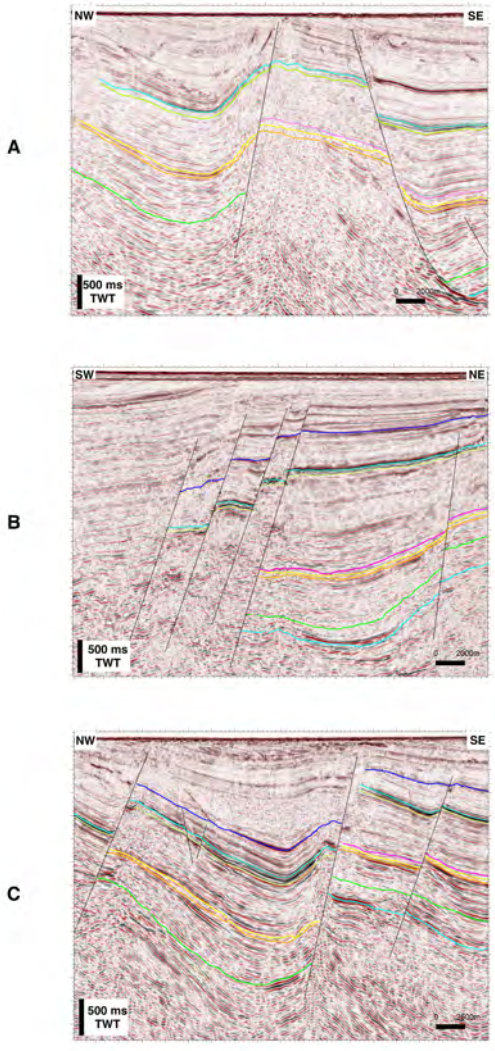

FIGURE 4.15: Segmentation of the Leirdjupet Fault Complex according to Gabrielsen et al. (1990). A - northern segment; B - central segment; C - southern segment.

Interpretation

It is clear that the Leirdjupet Fault Complex was active during numerous tectonic events. As mentioned earlier in the Chapter 2, Gabrielsen et al. (1990) suggested that main movements

took place in the (early?) Carboniferous, Mid Jurassic and Early Cretaceous. In addition, during later studies another faulting event was introduced to happen in the late Permian (?) (Gudlaugsson et al., 1998; Bjørnestad, 2012). Observed wedge-shape structures right below the interpreted horizon H3 of late Permian age and at the levels of BCU and Aptian ages are the direct indicator of tectonic movements. Potential wedge shape below horizon H2 of early Permian age and assumed H1 of mid Carboniferous, could support Gabrielsen et al. (1990) suggested tectonic movements in the (early?) Carboniferous. Dragging and folding structures detected were recognized by previous works (Gabrielsen et al., 1997; Bjørnestad, 2012; Dahlberg, 2014).

The Bjørnøyrenna Fault Complex

Description

The fault complex is oriented in the NE-SW direction and is represented by SE and NW dipping normal faults without dominating polarity, both synthetic and antithetic faults are present. Due to the erosion of the Loppa High it is difficult to determine the timing of faulting and displacement rates. However, potential wedge-shape indicating syntectonic deposition in the late Permian was detected in the southern part of the study area. It seems that the displacement is decreasing towards the north-east, where the Fingerdjupet Subbasin is located and is greater in the deeper horizons. Both, folding between main normal faults and dragging along their fault-plane are present.

Interpretation

Gabrielsen et al. (1990) suggested that the fault complex was tectonically active from the Late Triassic to early Cretaceous. In addition, potential wedge-shape of the late Permian was observed. Presence of much greater throws in the lower layers compared with the younger horizons indicate that the fault complex was more active earlier in the geological history, and later reactivated. In addition, the tectonic movements appear to have been greater in the southern part of the fault complex where throw was detected to be larger than in the northern part. Folding structures were previously documented (Dahlberg, 2014).

The fault complex separating the Fingerdjupet Subbasin from the Bjarmeland Platform

Description

The fault complex separating the Fingerdjupet Subbasin from the Bjarmeland Platform can be subdivided into three segments: southern, central and northern. The displacement is increasing

when going from the southern part towards north, and the highest values are reaches in the central part. In the northern part displacement decreases again. The southern segment is penetrated by one normal fault with strike orientation NNW-SSE dipping towards east and polarity of faulting mainly synthetic with minor faults terminating the main fault. The displacement is greater in the younger reflectors. The central part of the fault complex is contained of few normal synthetic faults and younger antithetic faults terminating them. The strike of faults shifts to N-S with dip towards west. The displacement is greater in the older horizons.

In the northern part of the fault complex, dipping direction is towards west and strike of faulting is NNE-SSW. The normal fault with younger antithetic faults terminating it is giving the structural trend of the segment with the displacement being the greatest in the older strata. The extent of the fault complex is the greatest in the northern segment. According to Dahlberg (2014), in the northern part of the fault complex, faults with E-W orientation are present and tend to have smaller offsets than the dominant faults striking NNW-SSE. The age of timing of the faults is difficult to determine due to erosion of most of the Cretaceous strata. However, faults with E-W direction are older than NNW-SSE trending faults and terminate against them (Dahlberg, 2014).

Interpretation

The subdivision of the fault complex into three distinct units with varying strike orientation and dip direction indicates the presence of graben-horst system and that it was active during several tectonic regimes. Different strike directions present in the fault complex could suggest that tectonic stresses, which were active in the area, had dissimilar orientation. This can be supported by the fault pattern striking E-W observed by Dahlberg (2014), which shows two completely different stress regimes. The greater extent of the fault complex in the northern part shows the tectonic regime to have been stronger here than compared with the central and southern parts. Varying displacement between the lower and upper strata at different fault complex segments indicates fault reactivation and changing stress intensity over the units.

4.4.2 Inner faults

Based on the set of 2D seismic lines main faults were interpreted in the Fingerdjupet Subbasin and are presented in Fig. 4.16. The dominant strike orientations of the inner faults in the study area are NNE-SSW, NE-SW, N-S or NW-SE. Several main fault patterns were observed while examining inner faults of the Fingerdjupet Subbasin: individual faults cutting only the horizon H1 of Carboniferous age; faults penetrating the whole interpreted succession from horizon H8

representing Aptian age and terminating right above the interpreted horizon H2 of Early Permian age; faults penetrating only horizon H5 of Middle Triassic age; and faults cutting through the whole interpreted succession from horizon H1 representing Carboniferous until horizon H8 indicating Aptian. Individual faults in the Fingerdjupet Subbasin detach at greater depths and have a listric nature.

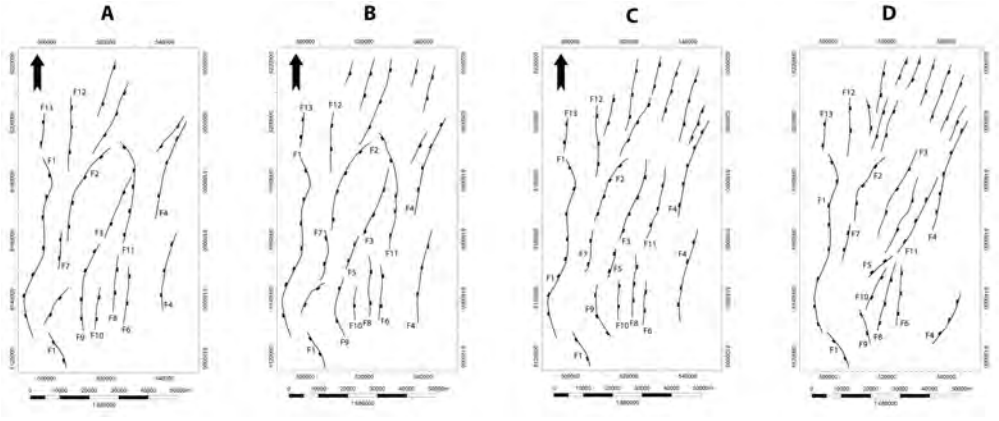

FIGURE 4.16: Interpreted faults in the Fingerdjupet Subbasin at four different levels. A - mid Carboniferous; B - early Permian; C - Middle Triassic; D - BCU.

As it can be seen in Fig. 4.16 the intensity of faulting is increasing going from mid Carboniferous to BCU, where the faulting is the densest. Moreover, dominant direction at the levels of mid Carboniferous, early Permian and Middle Triassic are NW-SE/NNW-SSE or N-S. While at the BCU level, faults in the southern part start to swing towards east. This could indicate changing orientation of the tectonic regime or that faults are following pre-existing relief. This might be the case in the western part of the Fingerdjupet Subbasin where fault orientation remain N-S at all 4 levels.

It is worth mentioning particular fault patterns present in the Fingerdjupet Subbasin and their features. One is penetrating the horizon H1 of mid Carboniferous age and terminating below the horizon H2 representing early Permian. However, this fault pattern does not generate syntectonic deposition thus indicating short duration tectonic regime. Therefore, approximate age of faulting could be interpreted as mid Carboniferous (Fig. 4.4).

Another fault pattern is initiating above the horizon H5 of Middle Triassic age and ceasing right below the horizon H2 indicating early Permian (Fig. 4.1). As it was mentioned in the key lines descriptions (Subchapter 4.1), limestones and evaporites act more ductile than overlying siliciclastic rocks and act as a decollement zone. Moreover, evaporites form the best decollement zones.

The third fault pattern is cutting the succession between H8 of Aptian age and terminating bellow the horizon H6 representing Top Upper Triassic (Fig. 4.1). This cessation can be explained by the short duration of tectonic regime or lithological effect. The Upper Triassic lithology (see Chapter 2) is mainly composed of interbedding shales and sandstones, which can be proven by the well-log data present from the three exploration wells in the Fingerdjupet Subbasin (7321/7-1; 7321/8-1; 7321/9-1). There, units of low gamma values indicating potential sandstone are interbedding with relatively high gamma readings having units representing shales. Therefore, it has been interpreted that units of shales act more ductile than sandstones and form more like a decollement zone preventing faults to penetrate deeper.

Chapter 5

Discussion

This chapter is a discussion about the Fingerdjupet Subbasin evolution and infill history based on previously presented results in Chapter 4. The discussion is subdivided into three main subchapters: 5.1 Basin infill history and controlling factors, dealing with the development of the three megasequences; 5.2 Evolution of the Fingerdjupet Subbasin in a regional context, where the geological history will be covered from the Caledonian basement until Late Triassic times; and the influence of the main bounding structural elements of the Fingerdjupet Subbasin separating it from the Bjørnøya Basin, will be discussed in 5.3 Leirdjupet and Bjørnøyrenna Fault Complexes.

5.1 Basin infill history and controlling factors

5.1.1 Megasequence 1 - MS1

The first interpreted megasequence has a varying thickness (150 – 675 ms) over the Fingerdjupet Subbasin (Fig. 4.11 A). MS1 contains minor wedge-shaped thickening of strata towards the inner faults (F6, F8, F9) of the subbasin in its southern part. The variation in thickness in the central and northern parts of the study area indicates that the previously formed structural relief was gradually infilled during the time of MS1 deposition in addition to infill of accommodation created by regional subsidence. Potential NNE-SSW lineaments in the time-thickness map (Fig. 4.11 A) might suggest presence of elongated areas with thickness variations. Such elongated areas of varied thickness may reflect variation in accommodation caused by the structural grain of the preexisting relief, or formed during the regional extension before, or during, the deposition of MS1.

Worsley (2008) interpreted a shift from continental to carbonate sedimentation in the Carboniferous (Chapter 2) after a regional uplift and subsequent rifting in local half-grabens and continued sea level rise. Based on this interpretation and the overall aggradational pattern of the megasequence, assumptions can be made that MS1 was onset during these events and

previous local highs and platforms were submersed. The strong amplitude reflections in the lower part of the MS1, with transition to weaker reflection pattern in the upper part of the megasequence (Fig. 4.11 B), are interpreted to reflect the change from cyclical dolomites and evaporites to massive limestones which took place in late Carboniferous to early Permian times in the Barents Sea-Svalbard region (Faleide et al., 2010). A cyclic variation between deposition of dolomite and evaporite suggests that high-frequency sea-level variations took place also in the Fingerdjupet Subbasin at the time of MS1 lower part deposition, as in other areas of the Barents Sea region.

According to Worsley (2008), a relatively abrupt transition from cyclical evaporite-dolomite to carbonate sedimentation indicates the end of the high – frequency rhythms in the sea level and the onset of second transgressive event. The carbonate deposition in the MS1 suggests that the Fingerdjupet Subbasin during the period from Carboniferous to Early Permian represented platform depositional environment and was more similar to the Bjarmeland Platform than the Bjørnøya Basin. Especially in the northern and southern part where no tectonic activity is recorded and the changes in thickness are minor.

In the southern part of the study area reflection pattern in the lower-middle part of MS1 changes from subparallel and parallel to divergent (Fig. 4.11 B). However, locally divergent reflection pattern is dominant throughout the whole MS1 and it extends even below the lower boundary of megasequence (Fig. 4.11 B). A change in the reflection pattern indicates a change from pre-tectonically controlled deposition into a phase where sedimentation was controlled by the creation of accommodation by tectonic movements. Presence of wedge-shape stratigraphic units in the hanging wall of faults (Fig. 4.3, 4.4, 4.5, faults F6, F8, F9) indicates that synsedimentary fault activity took place at the time of MS1 deposition in the southern part of the Fingerdjupet Subbasin. It is worth mentioning, that subsidence present in the central and northern parts of the study area might have been caused by the tectonic activity in the southern part.

As faults (4.4, 4.5, 4.6, faults F6, F8, F9), where wedge-shapes thicken towards their hanging-walls, are oriented N-S in the southern part of the study area (Subchapter 4.2), it can be predicted that extensional forces were oriented W-E direction when the faults were formed. The interpreted intrabasinal high (see key line 4 Fig. 4.4) might have been formed or already existed during the formation of MS1 and could support previously introduced idea of submersion of local highs and platforms. This assumption is based on differential thickness of strong reflections on the intrabasinal high and in the hanging-walls. The key observation for the interpretation is that the thickness of strong reflections is greater in the hanging-walls compared with the thickness on the intrabasinal high (Fig. 4.5 subareas G and E – hanging-walls, subarea F – intrabasinal high). Minor normal faults observed (Fig. 4.1, 4.5) throughout the study area penetrating

the lower boundary of the megasequence and terminating within the MS1, are indicating that regional extensional forces affected the Fingerdjupet Subbasin during the deposition of the MS1. However, these forces must have acted during a short period of time because no localized accommodation space and wedge-shapes were created.

5.1.2 Megasequence 2 - MS2

The thickness of MS2 varies much more (from 300 to 1250 ms) than the thickness of MS1 (Fig. 4.12). The lower part of the Megasequence 2, with subparallel to parallel reflection pattern and lack of onlaps, represents aggradation in a basin without any specific main depocenter (Fig. 4.12 B). Infilling of the paleo-relief that existed prior to the deposition of MS1 continued during regional subsidence by deposition of the lower part of the MS2. Earlier (see discussion of MS1) proposed platform depositional environment is believed to continue throughout the formation of the lower part of MS2.

The shift to the divergent reflection pattern in the central and southern parts is indicated by the presence of wedge-shaped units thickening towards the inner faults (F2 and F3) of the Fingerdjupet Subbasin (Fig. 4.1, 4.2) and footwall of the Loppa High (Fig. 4.13). This episode specifies the onset of the first localized depocenters in the area with faulting and subsidence. Two main depocenters were created during the deposition of the upper part of the MS2, with potential candidates in the south-eastern corner of the central depocenter, and in the southern part of the Fingerdjupet Subbasin. The thickness tends to be greater in the depocenter located in the central part of the Fingerdjupet Subbasin compared with the one located in the north-western part (Fig. 4.12 A). This may imply that extensional forces and movements along the fault-plane of F2 (Fig. 4.1) were greater in the central depocenter, where, a greater accommodation space was created than in the north-western depocenter. Faults bounding the central depocenter are orientated NNE-SSW and tend to follow the observed lineaments in the time-thickness map of MS1 (Fig. 4.11 A). The orientation of the faults indicates that the extensional force was oriented WNW-ESE or NW-SE during the time when MS2 was deposited.

An alternative interpretation for the arrangement of the depocenters of MS2 might be that the fault (F2) bounding the central depocenter followed the weakness zone formed between the basement block interpreted in key line 2 (Fig. 4.2, key line 2) and overlying strata, thus generating a bigger displacement and a greater accommodation space here.

As mentioned in Chapter 3, the succession from H3, representing late Permian, until H5, indicating Middle Triassic, thins out when going from the Bjarmeland Platform to the Fingerdjupet

Subbasin. This can be explained by either this succession is totally absent here or has a thickness below seismic resolution. If the thickness (36 meters of undifferentiated Fm in 7321/8-1 well) is below the seismic resolution then unit forms the upper part of MS2. The change from dominating carbonate deposition in late Carboniferous throughout the Permian to siliciclastic deposition in the Triassic might have occurred due to greatly increased regional subsidence rates in the Barents Sea, combined with input of terrigenous clastic material (Glørstad-Clark et al., 2010, 2011). The thinning out of the succession coming from the Bjarmeland Platform to the Fingerdjupet Subbasin might indicate that at the time of MS2 deposition the study area was located distant from the sediment source and/or a structural high was blocking sediments from coming in. This can explain the thin early post-rift unit or its absence.

5.1.3 Megasequence 3 - MS3

If the unit defined by horizon H3 of top Permian age and horizon H5 of Middle Triassic is thin (below seismic resolution) or absent in the Fingerdjupet Subbasin, then the boundary between the MS2 and MS3 indicates the shift from carbonate to siliciclastic sedimentation. The thickness of MS3 varies greatly, from 600 to 1450 ms (Fig. 4.14 A). The central depocenter, which existed in the MS2 time interval, had vanished, while the north-western depocenter had increased in extent. Moreover, a minor depocenter that existed in the south during deposition of MS2 extended significantly during the time infill of MS3 and represents the highest time-thickness values. Megasequence 3 does not thicken towards the hanging-walls of the faults F2 and F3 (Fig. 4.1, 4.2), thus indicating that the tectonic activity responsible for the formation of depocenters in "MS2-time" was over. Therefore, the MS3 is assumed to be a post-tectonic megasequence, deposited when the Fingerdjupet Subbasin still was continuing to subside due to previous tectonic activity, or due to post-extensional crustal cooling.

The separation of the megasequence into two parts suggests that it experienced two distinct depositional episodes. Strata with clinoforms prograding towards NW or NNW and downlapping the reflection situated right above the interpreted horizon H5 of Middle Triassic age, indicate that the sediment source was located in the SE or SSE of the study area (Fig. 4.14 B, C). Moreover, the surface that the clinoforms tend to downlap onto, could be interpreted as a maximum flooding surface, the depositional surface at the time when shoreline was at is maximum position landwards (Posamentier and Allen, 1999). Thus indicating that the sea level during the deposition of MS3 was relatively high. Clinoforms downlapping the reflection above the interpreted horizon H5 in the central and northern parts of the study area might indicate that at the time of MS3 deposition other parts of the Fingerdjupet Subbasin might have been

bounded by structural highs, which may have prevented sediments from coming into the basin. In addition, relatively oblique clinoform geometry with low angle and rather prominent topset (Fig. 4.14 C) could be interpreted as relatively muddy, low-energy regime (Mitchum Jr et al., 1977).

It has been interpreted that the southern depocenter was created during the tectonic extension that was initiated when the upper part of the MS2 was deposited. The lateral extent of the depocenter at that time might have been relatively similar to its extent during deposition of MS3 (Fig. 4.14 A). The fact that the thickness varies greatly from MS2 to MS3 within the same depocenter and that no syn-tectonic evidences were found in the MS3, suggest that during the timespan from the end of MS2 infill to the beginning of MS3 the depocenter was starving for sediments coming from the SE or SSE. This sediment route might have been blocked by the significantly uplifted Loppa High. This can be supported by the divergent reflection pattern in the southern part of the Fingerdjupet Subbasin during the timespan of MS2. Time had to pass until the basin to the east of the Loppa High was filled in and sediments were spilled over into the southern depocenter of the Fingerdjupet Subbasin.

The upper part of Megasequence 3 is represented by a subparallel to parallel reflection pattern, which suggests sedimentation from suspension in the basin during its gradual subsidence (Fig. 4.14 B). The reason why the central depocenter vanished and the extent of the north-western increased can be explained by the ceased local subsidence in the central part of the Fingerdjupet Subbasin and continuing subsidence in the north-western corner. A comparison of thicknesses between the two depocenters present in the MS3 suggests that differential subsidence was affecting the subbasin, and that the subsidence was greater in the southern part of the subbasin than in the north-western part, or the southern depocenter was starving for sediments.

Clinoforms present in the middle part of Megasequence 3 over the whole Fingerdjupet Subbasin (Fig. 4.14 B) does not form the same unit with the clinoforms downlapping surface interpreted as a maximum flooding surface (Fig. 4.14 C). They are separated with subparallel and parallel reflection pattern. This might indicate that sea level fluctuations have caused the possibility for sediments to be spilled over the potential bounding structural highs. The tangential oblique geometry of clinoforms in the middle part of the MS3 could represent a higher-energy slope system allowing coarse-grained sediments to be deposited in the foresets (Mitchum Jr et al., 1977; Veeken, 2007). Ideas explained above and clinoforms in the lower part of the MS3, which were interpreted to represent a relatively low-energy regime, support the idea of sea level fluctuations during the deposition of MS3. The successions with clinoforms in the northern and central parts of the Fingerdjupet Subbasin which have prograded from the NW or W (Fig. 4.14

D), could be interpreted to have been sourced from new structural highs created during the deposition of MS2 in the area west of the Fingerdjupet Subbasin.

NNE-SSW oriented lineaments (Fig. 4.14 A) indicate elongated areas of varying thickness parallel to faults. The lineaments occur in an area that mostly matches with the area of the graben structure width, as shown in the key lines 1 and 2 (Fig. 4.1, 4.2, subarea B2). The MS2 is within the graben structure greatly affected by faults that were initiating right above horizon H5 and terminating just below the horizon H2 and giving rise to a horst-graben topography. Therefore, it has been assumed that these faults were active during relatively short period of time (subchapter 4.4). Local and varying accommodation was created during the faulting in in MS2 along the faults, and this accommodation was later filled in during the deposition of MS3. This accommodation, created by the horst-graben topography, lead to thickness variations in areas elongated parallel to the faults, revealed in the time thickness map of MS3 (Fig. 4.14 A).

5.2 Evolution of the Fingerdjupet Subbasin in a regional context

5.2.1 Caledonian basement and Devonian extensional collapse

It is generally agreed, that most of the basement of the Barents Sea is of Caledonian origin (Gudlaugsson et al., 1998; Breivik et al., 2002, 2005; Ritzmann and Faleide, 2007). The faults oriented N-S in the south and along the western side of the Fingerdjupet Subbasin might indicate that they followed Caledonian basement relief (Fig. 4.16). This is in agreement with the interpretation of the new aeromagnetic data by Gernigon and Brönner (2012), which proposes that Caledonian basement orientation swings anticlockwise from the NE-SW trend in the southern part of the Finnmark Platform to NNW-SSE orientation through the Nordkapp Basin and into the Bjarmeland Platform (Fig. 5.2). NW-SE oriented anomalies (Fig. 5.2 A) are interpreted as nappes in arc-shaped Caledonian thrust. The Caledonian orogeny was followed by the Devonian extensional collapse, which is well documented in the Caledonides of southwestern Norway, and recognized in the Greenland and Scandinavian Caledonides (Fossen, 1992). Therefore, it can be assumed that the regional subsidence that is believed to influence the deposition of MS1 (see MS1 discussion) was directly caused by the Devonian extensional collapse.

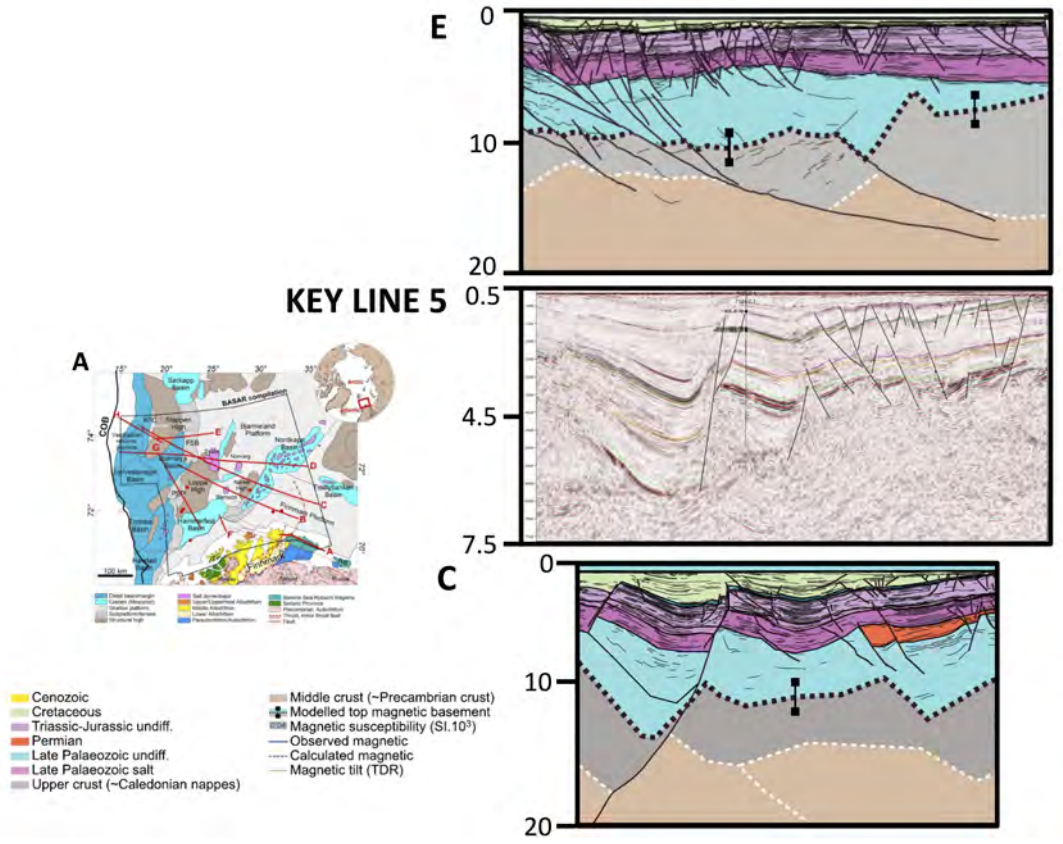

FIGURE 5.1: Two profiles crossing the northern (profile E) and southern (profile C) parts of the Fingerdjupet Subbasin where the black dashed line indicates and vertical bar errors indicate the depth estimation to top magnetic basement. A - structural framework of the SW Barents Sea. Red lines represent the location of profiles E and C. Key line 5 for comparison. Modified after Gernigon et al. (2014).

This brings up the idea that the strong reflectivity presented in Chapter 4 is probably caused by the basement block (Fig. 4.3, 4.4, 4.5), which could be of Caledonian origin and formed during the orogenic collapse and back-sliding. The age of wedge-shapes can be expected to be older than of Carboniferous age based on several factors. This includes assumed basement block of Caledonian age, dim reflections of potential wedge shapes (Fig. 5.3 and 5.4) and the great thickness between the basement block and in interpreted Carboniferous succession. Moreover, the faults bounding the wedge shapes have a different angle than faults penetrating younger interpreted strata and could indicate formation during different tectonic episode. The presence of a thick Late Paleozoic basin under the Fingerdjupet Subbasin can be supported by the work published recently by Gernigon et al. (2014), which based on aeromagnetic data implies thick strata of non-magnetic rocks overlying top basement surface but being older than Permian and Carboniferous successions interpreted during this study (Fig. 5.1).

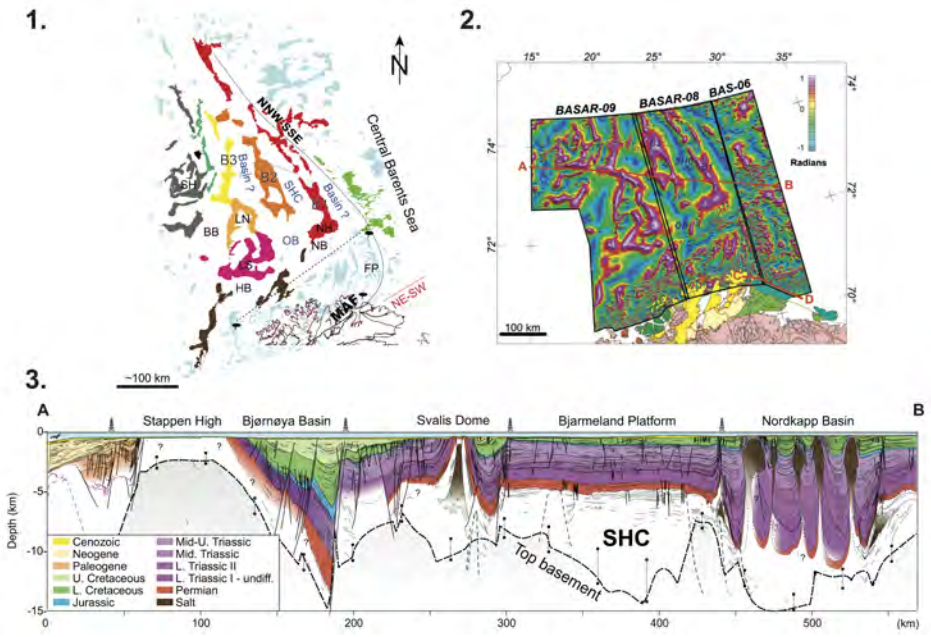

FIGURE 5.2: 1. Main highs observed from the aeromagnetic data at the present day in the SW Barents Sea; 2. Tilt-derivative filter applied on the recorded magnetic total field. The filter enhances the subtle magnetic anomalies and maximizes the geometrical contrasts of the internal basin structures. Note prominent NNW–SSE anomalies; 3. Regional NW–SE cross-section of the SW Barents Sea (line A–B). Modified after Gernigon and Brönner (2012).

This leads to a discussion that during the collapse of Caledonian orogen and backsliding, deep basins were formed in between the nappes and probably filled with sediments after eroding the Caledonian mountains. Therefore, observed wedge-shapes (Fig. 5.3 and 5.4) might represent Devonian sediments deposited during the Caledonian orogenic collapse in Devonian. This idea can be supported by the well known Devonian basins related to the post-orogenic collapse in surrounding areas like Svalbard, western and central Norway and in the Fjord Region of east Greenland (Braathen et al., 2002; Fossen, 2010; Piepjohn and Dallmann, 2014). However, the age of the observed wedge-shaped sequence is still under discussion and without well control at that depth in the area, the inferred ages are uncertain.

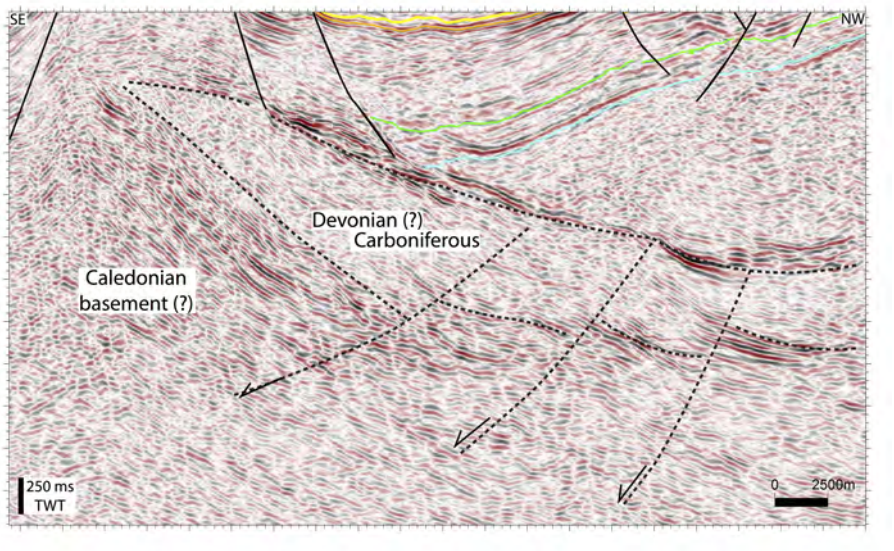

FIGURE 5.3: Close up of seismic key line 3. Dashed lines indicate potential faults cutting the basement block and sedimentary unit of Devonian (?) - Carboniferous rocks. For the full extent see Fig. 4.3.

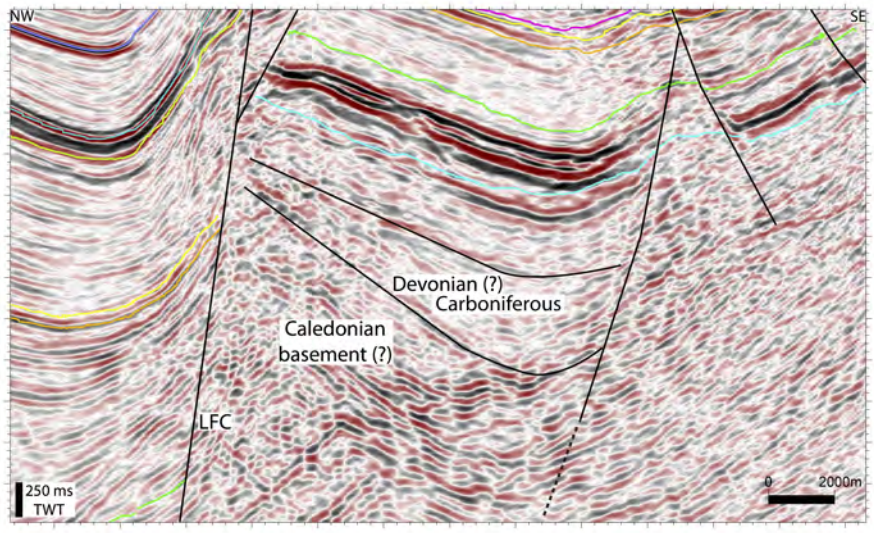

FIGURE 5.4: Close up of seismic key line 5. Note the outlined interpreted basement block and overlying wedge-shape of potential Devonian (?) - Carboniferous rocks. For the full extent see Fig. 4.5.

5.2.2 Carboniferous

During the Carboniferous an extensional event is recorded in the southern part (Fig. 4.3, 4.4, 4.5) of the Fingerdjupet Subbasin and is characterized by deposition of evaporites in the hanging walls. The exact age of the rifting in the southern part of the study area is hard to determine

due to the only assumed age of the horizon H1. However, it is believed to be a result of mid Carboniferous rifting. It is suggested by previous workers that the widespread rifting in the western Barents Sea occurred to the east of the Fingerdjupet Subbasin during mid Carboniferous and was coeval with tectonic activity in the Arctic and in the NE Atlantic rift systems (Doré, 1991; Faleide et al., 2008; Gudlaugsson et al., 1998). It is worth mentioning, that Gudlaugsson et al. (1998) interpreted the Fingerdjupet Subbasin as a westward tilted half-graben that formed in the hanging wall of basin bounding listric normal fault during the significant Late Palaezoic extension and is bounded by the intrabasinal horst in the south-east (Fig. 5.1). Moreover, the timing of the rifting can be supported by the work of Bugge and Fanavoll (1995) where Carboniferous is described with the deposition in half-grabens, which followed the mid Carboniferous rifting.

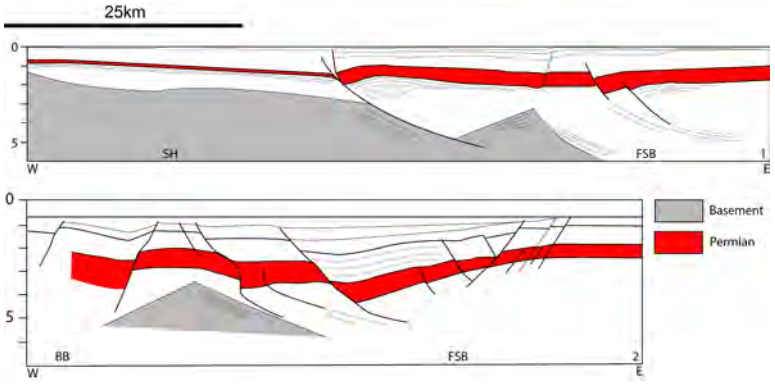

FIGURE 5.5: Interpreted sesmic profiles 1 and 2 from Stappen High and Fingerdjupet Subbasin. Location of profiles in the Fig. 5.6. SH - Stappen High, FB - Fingerdjupet Subbasin, BB - Bjørnøya Basin, LFC - the Leirdjupet Fault Complex. Modified after Gudlaugsson et al. (1998).

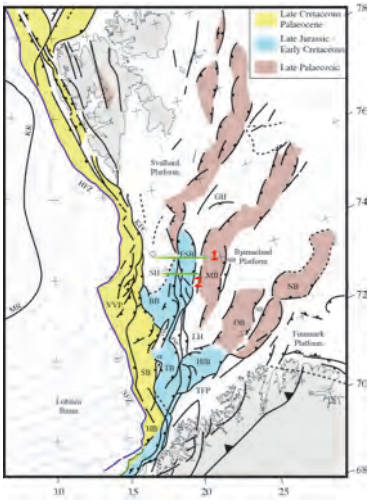

FIGURE 5.6: Regional map of the SW Barents Sea. Green lines indicate location of profiles in Fig. 5.5. Modified after Faleide et al. (2010).

However, mid Carboniferous rifting did not propagate to the central and northern parts of the study area thus indicating depositional environment on a stable platform. This matches with the idea suggested by Larssen et al. (2002) that the deposition occurred on platforms and basins with stable structural conditions and uniform sediment thickness. Therefore, the local subsidence that has influenced the central and northern parts of the study area during the deposition of MS1 might have been a response to the active rifting in the south (see MS1 discussion). Moreover, faults penetrating horizon H1 and terminating within the MS1 throughout the central and northern parts of the Fingerdjupet Subbasin (Fig. 4.3 and 4.4) might be response to the active rifting in the south as well.

The potential NE-SW lineaments in the time-thickness map of MS1 (Fig. 4.11, A), might indicate the orientation of mid Carboniferous rifting and suggest that the stress regime was oriented NW-SE direction. It would match with the idea that the fan-shaped array of rift basins and intrabasinal highs in the western Barents Sea with a dominant NE-SW trend, formed the restricted circulation depositional environment for evaporites to deposit (Gudlaugsson et al., 1998; Ritzmann and Faleide, 2007; Faleide et al., 2008, 2010).

The assumed age of horizon H1 and wedge-shapes extending above and below the selected reflector brings up the debate of initiation of the Selis Ridge in late Moscovian (late Carboniferous) due to the uplift along the Jason Fault Complex, proposed by Glørstad-Clark et al. (2011), and reaching the southern part of the Fingerdjupet Subbasin. Supporting idea could be that a half-graben area was created in the east of the southern part of the Selis Ridge, where evaporites deposited and subarea E (Fig. 4.3 4.4, 4.5 and 4.6) might have been the continuation of it (Glørstad-Clark et al., 2011). Another supporting idea could be the intrabasinal high (Fig. 4.4, 4.5, subarea F) which was interpreted to form during mid Carboniferous rifting.

The high-frequency sea level fluctuations and the second transgressive event discussed in the 5.1.1 Megasequence MS1 might be caused by the glacio-eustacy introduced by Stemmerik and Worsley (2005), where they state that the deposition during the late Carboniferous and early Permian was highly influenced by the regional glacio-eustacy influenced by the changing subsidence rates due to development of the Uralide orogeny and glaciation-deglaciation of Gondwana.

5.2.3 Permian

The early Permian in the Fingerdjupet Subbasin can be described as a tectonically quite period. The area experienced subsidence and the lower part of MS2 represents aggradation (see 5.1.2 Megasequence 2 - MS2), which was probably a result of continuing formation of a regional sag

basin in the Barents Sea caused by the post-rift subsidence after Carboniferous rifting. The main depocenter at that time was located in the eastern Barents Sea (Gudlaugsson et al., 1998; Nøttvedt et al., 2013).

Syntectonic deposition was recorded by wedge-shapes below horizon H3 of Capitanian age in the central and southern parts of the Fingerdjupet Subbasin where depocenters created in MS2 show the establishment of a new tectonic event. The thickness of MS2 on the intrabasinal high (Fig. 4.3, subarea D) is thinner compared to the thickness in the hanging-wall (Fig. 4.3, subarea D) and indicates that the intrabasinal high was uplifted during late Permian times. In addition faults below the structural high (Fig. 4.1, 4.2 and 4.3, subarea C) interpreted to be of late Permian age are supporting the idea of uplift in the Fingerdjupet Subbasin during the late Permian. It is worth mentioning that the interpreted basement high (Fig. 4.3, key line 3) geometry is fairly similar to the geometry of the Selis Ridge (Fig. 5.6). Therefore, it is reason to believe that the Selis Ridge, which according to Glørstad-Clark et al. (2011) was reactivated during the late Permian, potentially continued north into the southern and central parts of the Fingerdjupet Subbasin. Gabrielsen et al. (1990) proposed that the Fingerdjupet Subbasin was formed in Early Cretaceous. Based on the observation described above it can be proposed that initiation of the basin started during the late Permian (Capitanian).

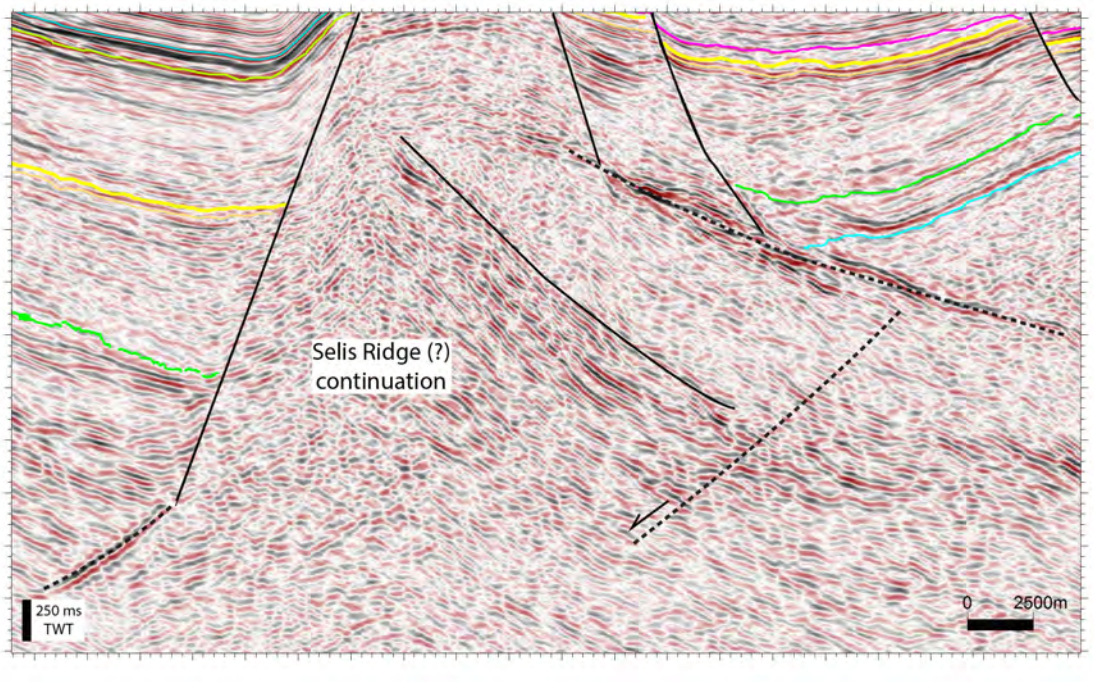

FIGURE 5.7: Close up of the seismic key line 3. Note the outlined basement block and its similarities to the Selis Ridge in Fig. 5.8.

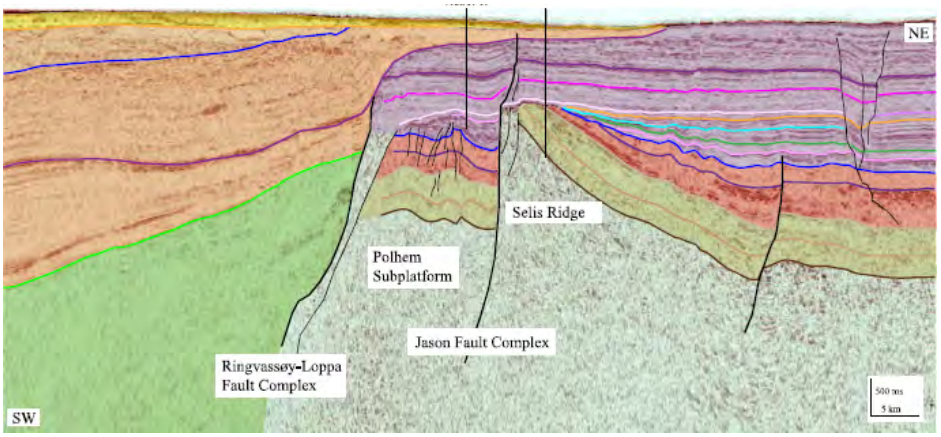

FIGURE 5.8: Paleo- and Loppa High western boundary fault complexes(Glørstad-Clark et al., 2011). Note the similarities in geometry of the Selis Ridge and the basement block in Fig. 5.7.

The Late Permian tectonic activity in the southern and central parts of the Fingerdjupet Subbasin was possibly linked to renewed extension in the North Atlantic region. The tectonic activity propagated northwards and was likely the main cause for the footwall uplift of the paleo-Loppa and Stappen highs (Gabrielsen et al., 1990; Gudlaugsson et al., 1998; Ziegler, 1988). The rifting mainly acted along north trending structures located in the western part of the rift system. Therefore, it was restrained in the other parts of the Barents Sea, because the main deformation was concentrated in the area where link between the northeast Atlantic and Arctic rifts was initiated (Gudlaugsson et al., 1998). It is worth mentioning that the N-S trending ridge proposed by Gudlaugsson et al. (1998) could be reflected in the time-structure map (Fig. 4.8) where faults in the southern part tend to be oriented N-S.

The sequence of several uplifting events during Permian is a potential reason why the southern depocenter in the Fingerdjupet Subbasin extended significantly during MS3 compared with MS2 (Fig. 4.14 and 4.14). During a relatively short period of time (from Kungurian to the latest Permian) the Selis Ridge experienced two uplifting events thus forming great sediment barrier and could support the idea of depocenter creation in the southern part of the study area during the end of MS2 and its starvation for the sediments later during Early Triassic. Moreover, this would support the condensed or absent immediate post-rift unit.

5.2.4 Triassic

The Triassic in the Fingerdjupet Subbasin can be characterized as a tectonically calm period when the accommodation space was controlled by the regional subsidence probably related to crustal cooling after late Permian rifting in the North Atlantic region.

Throughout the Triassic unit in the study area, progradational directions of sedimentary packages to NW-NNW, SE or SW show varying sediment source. During the Early Triassic times rifting was present in the area between Norway and Greenland and Uralian orogeny culminated in the east during the Early Triassic (Gudlaugsson et al., 1998; Müller et al., 2005). This would suggest that the potential source from the southeast was Uralian mountains. Moreover, the Fennoscandian Shield was situated in the south and could have acted as a sediment source as well. It is believed, that the Fennoscandian Shield together with Uralian mountains were the main sediment sources for prograding sedimentary packages towards the NW-NNW in the lower and middle parts of the MS3 (5.1.3 Megasequence 3 – MS3). However, local source areas cannot be excluded, like Novaya Zemlya to the east, which may have acted as a more prominent sediment source in Middle-Late Triassic (Buiter and Torsvik, 2007; Smelror et al., 2009).

Sedimentary packages in the upper part of MS3 prograding SE indicate abrupt change in the direction of sediment infill during Late Triassic. Prograding systems from the west to the east are recorded on the Loppa High in the middle Ladinian and during Late Triassic thus supporting new sediment source to the west of the Fingerdjupet Subbasin. One potential source for these progradational systems might have been Stappen High or rifted fault block to the west of the Fingerdjupet Subbasin (Doré, 1991; Ziegler, 1988). Moreover, Greenland was located to the west and is believed to represent the main sediment source for the Upper Triassic succession (Glørstad-Clark et al., 2010). The signifying fact is that the Loppa High is located to the southeast of the Fingerdjupet Subbasin and the sedimentary packages prograding from NW must have passed the study area before they were finally deposited in the Loppa High area. Therefore, it can be concluded that Greenland, Stappen High or individual rifted fault block to the west of the study area might have sourced prograding system from the NW in the northern part of the Fingerdjupet Subbasin.

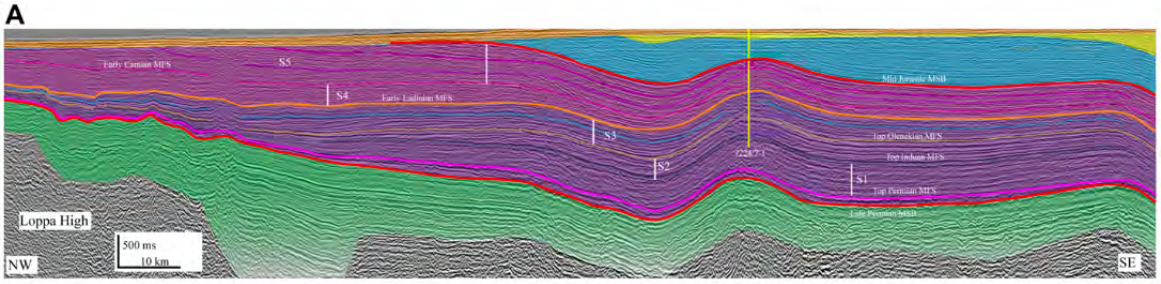

FIGURE 5.9: Southeast to northwest trending seismic line towards paleo-Loppa High displaying the Triassic succession (Glørstad-Clark et al., 2010). For the location of the seismic line see Fig. 5.10.

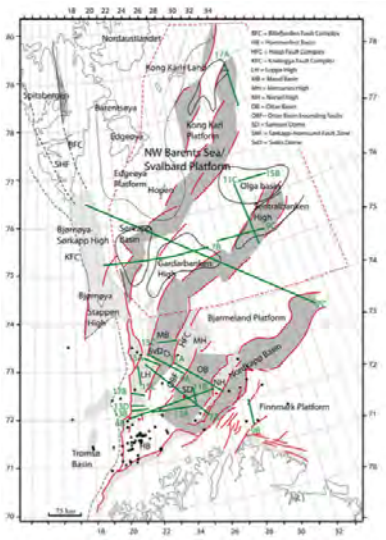

FIGURE 5.10: Late Paleozoic tectonic element map the western Barents Sea. The red dashed line denotes the NW Barents Sea area. Location of the seismic line in Fig. 5.10 is marked with the red line and index 7A (Glørstad-Clark et al., 2010).

The cross-section showing Triassic succession subdivision in sequences across the SW Barents Sea by Glørstad-Clark et al. (2011) can be seen in Fig. 5.9 with the location of the seismic line indicated in Fig. 5.10. The unit comprising sequences S4 and S5 (Early Ladinian – Mid Jurassic) fairly coincides with the MS3 defined in the Fingerdjupet Subbasin, taking into account that the thickness of the unit between horizons H3 and H5 is below the seismic resolution. The combined thickness of S4 and S5 on the western side of the cross-section reaches ca. 1300 ms (Fig. 5.9). Considering the fact that the Loppa High was uplifted and eroded in the Late Jurassic – earliest Cretaceous, it can be assumed that the Loppa High, together with the southern part of the Fingerdjupet Subbasin where thickness in MS3 varies from 800-1500 ms (Fig. 4.14 A), formed a depocenter during the Late Triassic. After the Selis Ridge was transformed from a structural high into a basin during late Triassic times (Faleide et al., 1984; Gabrielsen et al., 1990). The same change is recognized in the Bjørnøya-Sørkapp High, which became a depocenter in Late Triassic (Gabrielsen et al., 1990; Gudlaugsson et al., 1998). This change from uplift to subsidence required substantial change in the stress regime. The cause of it is still under discussion, but is believed to be due to renewed crustal extension in the North Atlantic region between Norway and Greenland (Ziegler, 1988; Glørstad-Clark et al., 2010).

5.3 Leirdjupet and Bjørnøyrenna Fault Complexes

The Leirdjupet Fault Complex separates the Fingerdjupet Subbasin from the main Bjørnøya Basin. Based on the observations it can be concluded that the Leirdjupet Fault Complex was

active during at least three discrete phases: late Permian, Late Jurassic – earliest Creataceous, and Aptian. In addition there is also a potential syntectonic deposition of predicted Carboniferous age.

Interestingly, interpreted wedge-shape in the Carboniferous succession is located along the southern part of the Fingerdjupet Subbasin where syntectonic deposition is recognized along the inner faults. Thus bringing into the discussion, that this tectonic episode might be simultaneous and supporting the idea of the Selis Ridge propagation north into the southern part of the Fingerdjupet Subbasin. Moreover, based on wedge-shapes of interpreted late Permian time, the Leirdjupet Fault Complex was active along the whole western side of the Fingerdjupet Subbasin. With the support of wedge-shapes, interpreted to be of late Permian age, present in the southern part of the study area along the northern part of the Bjørnøyrenna Fault Complex and in the central part where syndepositional tectonics is recognized along the inner faults.

Assuming activity of the Selis Ridge along the Leirdjupet and Bjørnøyrenna fault complexes in the Carboniferous and late Permian it can be proposed that these fault complexes are bounding the western side of the Selis Ridge continuation. This could make the Leirdjupet and Bjørnøyrenna fault complexes having regional significance and support the idea of (Barrère et al., 2009) where it was considered that previously mentioned fault complexes together with the Ringvassøy-Loppa Fault Complex are linked to the Billefjorden Fault Zone in Svalbard, and that they are all related to a Caledonian deep-seated weak zone. This can be supported by the new aeromagnetic data interpreted by (Gernigon et al., 2014), where previously mentioned fault complexes are following N-S elongated anomalies in the magnetic field (Fig. 5.6). Moreover, this could be supported by Gabrielsen et al. (1990) where the potential tectonic episode from the latest Carboniferous to Permian was proposed. After examining the throws of the Leirdjupet Fault Complex along the western side of the Fingerdjupet Subbasin, it can be assumed that the faulting was propagating northwards where the throw is interpreted to be lower. Both, Late Jurassic - earliest Cretaceous and Aptian wedge-shapes in the Fingerdjupet Subbasin and along the Leirdjupet Fault Complex indicate that both tectonic episodes acted on two separate structural elements. These wedge-shapes were previously described in other works (Faleide et al., 1993b,a; Bjørnestad, 2012; Dahlberg, 2014).

The folding along the Leirdjupet Fault Complex might be related to transpressional stress, which can be linked to the contraction, which acted on the Bjørnøyrenna Fault Complex in the Late Cretaceous – Early Tertiary (Gabrielsen et al., 1997). Based on the same work by Gabrielsen et al. (1997), inversion acted in the Hauterivian – Aptian in the Bjørnøya Basin and is believed to be of semi-regional scale and may also have affected both the Leirdjupet Fault

Complex and Fingerdjupet Subbasin. According to Dahlberg (2014), it might have resulted in a more extensive subsidence, folding and structural highs in the Fingerdjupet Subbasin.

It was described in the Chapter 2, where current half-graben geometry observed in the Bjørnøya Basin is considered to be the true galf-graben geometry or a secondary effect of inversion of the Stappen High. After this study, based on potential tectonic activity of the Bjørnøya Basin in Carboniferous and rifting in the late Permian it can be suggested that it is a true half-graben geometry inherited after the response to several rifting events. It can be supported by Gernigon et al. (2014) proposed V-shaped, low magnetic anomaly, which coincides with the present outline of the Bjørnøya Basin lying between two noticeable high magnetic domains defined by the Stappen and Loppa Highs (Fig. 5.2 and 5.1). The magnetic anomaly indicates deep top basement thus suggesting a deep basin beneath the present Bjørnøya Basin. Therefore, it brings the question if the formation of the deep basin was related to the Devonian (?) extension caused by the collapse and backsliding of the Caledonian nappes. However, due to the great depth and seismic resolution loss this is hard to determine.

Chapter 6

Conclusions

The pre-Jurassic geological evolution of the Fingerdjupet Subbasin reveals complex interaction between sedimentation and tectonics. During Paleozoic times the Fingerdjupet Subbasin experienced three rifting events: Devonian (?), mid-Carboniferous and late Permian. It is clear that the geological evolution is closely linked with the sequential uplifting events of the Selis Ridge. Devonian (?) rifting might be related with the collapse of the Caledonian orogen and its interpretation is supported by aeromagnetic data indicating potential deep Devonian (?) basins beneath the present Fingerdjupet Subbasin. Both mid Carboniferous and late Permian rifting events are associated with reactivated extension in the North Atlantic and Arctic regions. The local subsidence in the southern part of the Fingerdjupet Subbasin is believed to be a consequence of mid Carboniferous rifting that acted in a wide area of the western and central Barents Sea. Variations in extent of Permian depocenters were controlled by differential subsidence and ceased tectonic extension. During the Early to Mid Triassic the Fingerdjupet Subbasin was starving for sediments due the sequential uplifting of the Selis Ridge in late Permian, while in Late Triassic it became a part of the regional sag basin. The main events in the geological evolution of the Fingerdjupet Subbasin from Carboniferous until Late Triassic are these:

1. Potential deep basin related to the Devonian (?) extension caused by collapse of Caledonian orogen is situated below the Late Paleozoic strata.

2. Mid Carboniferous rifting acted in the southern part as a result of extensional tectonics in the North Atlantic and Arctic regions.

3. The Selis Ridge potentially continued up north during the mid Carboniferous and late Permian times to the southern and central parts of the Fingerdjupet Subbasin.

4. North Atlantic and Arctic extension is recorded in the central and southern parts of the Fingerdjupet Subbasin in late Permian (Capitanian).

5. Southern part of the study area was included in the paleo Loppa High depocenter during Late Triassic.

6. Sediments in the Upper Triassic unit were derived from several source areas. Potentially from Uralian orogen and Fennoscandian Shield in the southeast and Greenland to the west.

Bibliography

Barrère, C., Ebbing, J., and Gernigon, L. (2009). Offshore prolongation of Caledonian structures and basement characterisation in the western Barents Sea from geophysical modelling. *Tectonophysics*, 470(1):71–88.

Bjørnestad, A. (2012). Structural analysis of the Leirdjupet Fault Complex in the southwestern Barents Sea. Master's thesis, University of Oslo, Norway.

Braathen, A., Osmundsen, P. T., Nordgulen, O., Roberts, D., and Meyer, G. B. (2002). Orogen-parallel extension of the Caledonides in northern Central Norway: an overview. *Norsk Geologisk Tidsskrift*, 82(4):225–242.

Breivik, A. J., Mjelde, R., Grogan, P., Shimamura, H., Murai, Y., and Nishimura, Y. (2005). Caledonide development offshore–onshore Svalbard based on ocean bottom seismometer, conventional seismic, and potential field data. *Tectonophysics*, 401(1):79–117.

Breivik, A. J., Mjelde, R., Grogan, P., Shimamura, H., Murai, Y., Nishimura, Y., and Kuwano, A. (2002). A possible Caledonide arm through the Barents Sea imaged by OBS data. *Tectonophysics*, 355(1):67–97.

Bugge, T. and Fanavoll, S. (1995). The Svalis Dome, Barents Sea-a geological playground for shallow stratigraphic drilling. *First break*, 13(6).

Buiter, S. J. and Torsvik, T. H. (2007). Horizontal movements in the eastern Barents Sea constrained by numerical models and plate reconstructions. *Geophysical Journal International*, 171(3):1376–1389.

Dahlberg, M. E. (2014). Structural and stratigraphical evolution of the Fingerdjupet Subbasin, SW Barents Sea.

Dalland, A., Worsley, D., and Ofstad, K. (1988). *A Lithostratigraphic Scheme for the Mesozoic and Cenozoic and Succession Offshore Mid-and Northern Norway.* Oljedirektoratet.

Doré, A. (1991). The structural foundation and evolution of Mesozoic seaways between Europe and the Arctic. *Palaeogeography, Palaeoclimatology, Palaeoecology*, 87(1):441–492.

Doré, A. (1995). Barents Sea geology, petroleum resources and commercial potential. *Arctic*, pages 207–221.

Faleide, J. I., Bjørlykke, K., and Gabrielsen, R. H. (2010). Geology of the Norwegian continental shelf. In *Petroleum Geoscience*, pages 467–499. Springer.

Faleide, J. I., Gudlaugsson, S. T., and Jacquart, G. (1984). Evolution of the western Barents Sea. *Marine and Petroleum Geology*, 1(2):123–150.

Faleide, J. I., Tsikalas, F., Breivik, A. J., Mjelde, R., Ritzmann, O., Engen, O., Wilson, J., and Eldholm, O. (2008). Structure and evolution of the continental margin off Norway and the Barents Sea. *Episodes*, 31(1):82.

Faleide, J. I., Vågnes, E., and Gudlaugsson, S. T. (1993a). Late Mesozoic-Cenozoic evolution of the south-western Barents Sea in a regional rift-shear tectonic setting. *Marine and Petroleum Geology*, 10(3):186–214.

Faleide, J. I., Vågnes, E., and Gudlaugsson, S. T. (1993b). Late Mesozoic-Cenozoic evolution of the southwestern Barents Sea. *Geological Society, London, Petroleum Geology Conference series*, 4:933–950.

Fossen, H. (1992). The role of extensional tectonics in the Caledonides of south Norway. *Journal of structural geology*, 14(8):1033–1046.

Fossen, H. (2010). *Structural geology*. Cambridge University Press.

Gabrielsen, R. (1984). Long-lived fault zones and their influence on the tectonic development of the southwestern Barents Sea. *Journal of the Geological Society*, 141(4):651–662.

Gabrielsen, R. H., Faerseth, R. B., and Jensen, L. N. (1990). *Structural Elements of the Norwegian Continental Shelf. Pt. 1. The Barents Sea Region*. Norwegian Petroleum Directorate.

Gabrielsen, R. H., Grunnaleite, I., and Rasmussen, E. (1997). Cretaceous and tertiary inversion in the Bjørnøyrenna Fault Complex, south-western Barents Sea. *Marine and Petroleum Geology*, 14(2):165–178.

Gernigon, L. and Brönner, M. (2012). Late Palaeozoic architecture and evolution of the south-western Barents Sea: insights from a new generation of aeromagnetic data. *Journal of the Geological Society*, 169(4):449–459.

Gernigon, L., Brönner, M., Roberts, D., Olesen, O., Nasuti, A., and Yamasaki, T. (2014). Crustal and basin evolution of the southwestern Barents Sea: from Caledonian orogeny to continental breakup. *Tectonics*, 33(4):347–373.

Glørstad-Clark, E., Birkeland, E., Nystuen, J., Faleide, J., and Midtkandal, I. (2011). Triassic platform-margin deltas in the western Barents Sea. *Marine and Petroleum Geology*, 28(7):1294–1314.

Glørstad-Clark, E., Faleide, J. I., Lundschien, B. A., and Nystuen, J. P. (2010). Triassic seismic sequence stratigraphy and paleogeography of the western Barents Sea area. *Marine and Petroleum Geology*, 27(7):1448–1475.

Gudlaugsson, S., Faleide, J., Johansen, S., and Breivik, A. (1998). Late Palaeozoic structural development of the south-western Barents Sea. *Marine and Petroleum Geology*, 15(1):73–102.

Høy, T. and Lundschien, B. (2011). Triassic deltaic sequences in the northern Barents Sea. *Geological Society, London, Memoirs*, 35(1):249–260.

Johansen, S., Ostisty, B., Birkeland, Ø., Fedorovsky, Y., Martirosjan, V., Christensen, O. B., Cheredeev, S., Ignatenko, E., and Margulis, L. (1993). Hydrocarbon potential in the Barents Sea region: play distribution and potential. volume 2 of *Norwegian Petroleum Society Special Publications*, pages 273 – 320. Elsevier.

Larssen, G., Elvebakk, G., Henriksen, L. B., Kristensen, S., Nilsson, I., Samuelsberg, T., Svånå, T., Stemmerik, L., and Worsley, D. (2002). Upper Palaeozoic lithostratigraphy of the southern Norwegian Barents Sea. *Norwegian Petroleum Directorate Bulletin*, 9:76.

Mitchum Jr, R., Vail, P., and Sangree, J. (1977). Seismic stratigraphy and global changes of sea level: Part 6. Stratigraphic interpretation of seismic reflection patterns in depositional sequences: Section 2. Application of seismic reflection configuration to stratigraphic interpretation.

Müller, R., Ngstuen, J. P., Eide, F., and Lie, H. (2005). Late Permian to Triassic basin infill history and palaeogeography of the Mid-Norwegian shelf—East Greenland region. *Norwegian Petroleum Society Special Publications*, 12:165–189.

Norwegian Petroleum Directorate (2015). Norwegian Petroleum Directorate fact pages.

Nøttvedt, A., Cecchi, M., Gjelberg, J., Kristensen, S., Lønøy, A., Rasmussen, A., Rasmussen, E., Skott, P., and Van Veen, P. (2013). Svalbard-Barents Sea correlation: a short review. *Arctic Geology and Petroleum Potential, Norwegian Petroleum Society (NPF), Special Publication*, 2:363–375.

Piepjohn, K. and Dallmann, W. K. (2014). Stratigraphy of the uppermost Old Red Sandstone of Svalbard (Mimerdalen Subgroup). *Polar Research*, 33.

Posamentier, H. W. and Allen, G. P. (1999). Siliciclastic sequence stratigraphy: concepts and applications.

Riis, F., Lundschien, B. A., Høy, T., Mørk, A., and Mørk, M. B. E. (2008). Evolution of the Triassic shelf in the northern Barents Sea region. *Polar Research*, 27(3):318–338.

Ritzmann, O. and Faleide, J. I. (2007). Caledonian basement of the western Barents Sea. *Tectonics*, 26(5).

Rønnevik, H. and Jacobsen, H.-P. (1984). *Structural highs and basins in the western Barents Sea*. Springer.

Smelror, M., Petrov, O., Larssen, G. B., and Werner, S. (2009). Geological history of the Barents Sea. *Norges Geol. undersøkelse*, pages 1–135.

Stemmerik, L. and Worsley, D. (2005). 30 years on: Arctic Upper Palaeozoic stratigraphy, depositional evolution and hydrocarbon prospectivity. *Norsk Geologisk Tidsskrift*, 85.

Veeken, P. (2007). Seismic stratigraphy. Basin analysis and Reservoir characterization, Vol. 37.

Worsley, D. (2008). The post-Caledonian development of Svalbard and the western Barents Sea. *Polar Research*, 27(3):298–317.

Ziegler, P. A. (1988). Evolution of the Arctic-North Atlantic and the Western Tethys. A visual presentation of a series of paleogeographic-paleotectonic maps. *AAPG memoir*, 43:164–196.